Enhancement of durability by silica coating Pt-based catalysts for fuel cell application

シリカ被覆技術を用いた燃料電池用白金系触媒の耐久性向上

Wattanachai YAOWARAT

2016

Department of Material Science and Engineering

Graduate School of Engineering

Nagoya University

~ *Table of Contents* ~

Chapter 1

~ Introduction ~

~ Introduction ~

1.1 Motivations

Emissions from fossil fuels combustion for transportation and generate electricity substantially contribute to air pollution, especially the increasing of greenhouse gas concentration in the atmosphere. The consequences are human health problems, damage of ecological, plants, and global warming. The greenhouse effect is induced by greenhouse gases such as carbon dioxide (CO_2), nitrous oxide (N_2O), and methane (CH_4) in the atmosphere. CO_2 is the results of combustion of fossil fuels. Besides CO_2 and water (H_2O), the combustion products contain carbon monoxide (CO), nitrogen oxides (NO_x), and unburned hydrocarbons, all of these gases are toxic to human health, plants, and animals.

Since global concerns about the environment and human health, cleaner fuels and more effective energy conversion technologies are developed. Fuel cells are developed which change hydrogen and oxygen (oxidant) by chemical reaction into electrical energy. There are many types of fuel cells; this work is focused for proton exchange membrane fuel cell (PEMFC) application. PEMFC has many advantages because low temperature operation is available, low emissions are generated from this device and this reaction convert to electrical energy with high efficiency [1,2]. In the present, it is well known that the Pt supported on carbon materials are used be commercially catalyst in PEMFC. The excellent electrocatalyst for cathode electrode should well disperse on material supports in nano size to achieve the highest active sites of electrocatalyst which affect to high activities of oxygen reduction reaction (ORR) per mass of electrocatalyst. Moreover, the durability of electrocatalyst in acidic conditions on the cathode electrode also is concerned under operation of fuel cell [3]. The degradation phenomena of catalyst in fuel cell can occur such as Platinum dissolved in acidic electrolyte, Pt nanoparticles moved to together each others to form big particles, Pt nanoparticles removed from carbon support and Ostwald ripening [4].

In this study, silica was synthesized to cover Pt-based catalysts (1) to avoid the agglomeration of the Pt nanoparticles and (2) to prevent Pt nanoparticles removed from carbon supports. This study is expected to provide an alternative solution for high durability electrode material for PEMFC.

1.2 Fuel Cells

The Devices which Electrical energy directly generated from fuels and oxidants by chemical reaction are called "Fuel cells". It is an excellent alternative electrical generator which produces low emissions and high efficient electrical conversion. The components of fuel cell or cell unit compose of three parts 1) electrolyte layer, 2) porous anode electrode and 3) porous cathode electrode. Fig. 1.1 shows components and flow directions of fuel, oxidant and ions.

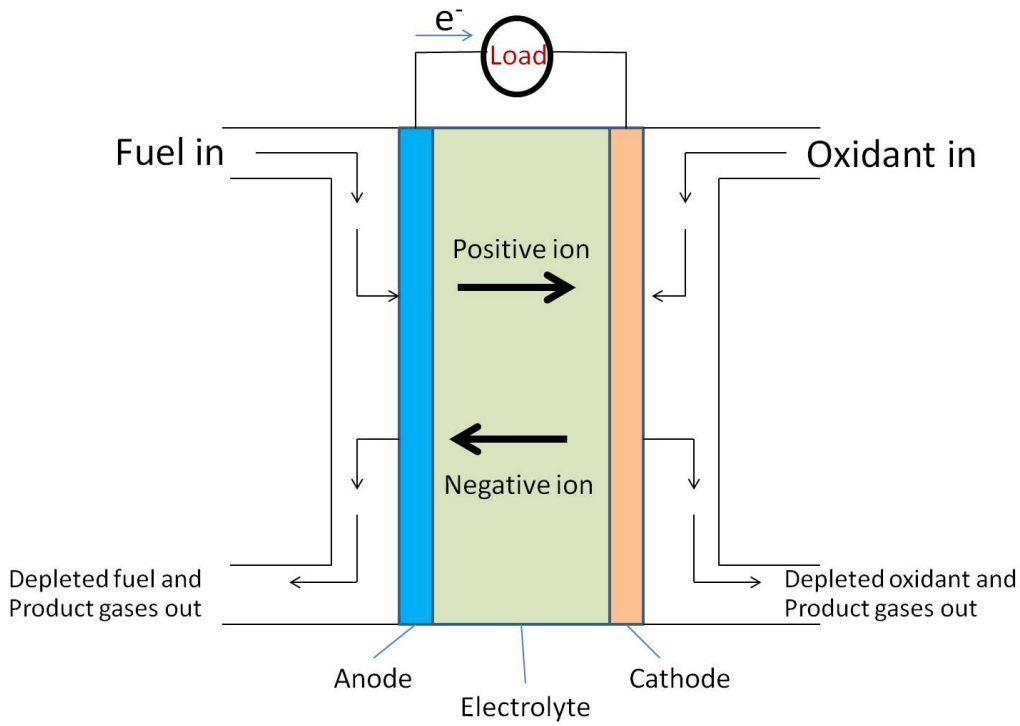

Fig. 1.1 Components and flow directions of Fuel cell

In fuel cell operation, the electrical is generated by electrochemical reaction between fuel and oxidant which are fed in anode electrode and cathode electrode, respectively. The residue fuel and oxidant leave from anode electrode and cathode electrode, respectively. The electrons pass through electrolyte from cathode electrode to anode electrode to perform work at load. Fuel cells are often categorized by the type of electrolyte. This is determined by the type and purity of the fuel, oxidant used and the operating temperature. Nowadays, six types of fuel cell were well developed as shown below [5]:

♣ Proton exchange membrane fuel cell (PEMFC)

♣ Alkaline fuel cell (AFC)

♣ Direct methanol fuel cell (DMFC)

♣ Phosphoric acid fuel cell (PAFC)

♣ Molten carbonate fuel cell (MCFC)

♣ Solid oxide fuel cell (SOFC)

The detail of six types of fuel cell was reported in references [6,7]. The types of fuel cell are summarized in table 1.

Fuel cell type	**Electrolyte used**	**Catalyst**	**Operating temp., °C**	**Electrode reaction**
Proton exchange membrane	Proton exchange membrane	Pt on anode and cathode	60-140	Anode: $H_2=2H++2e^-$ Cathode:$1/2O_2+2H^++2e^-=H_2O$
Alkaline	Potassium hydroxide	Non-precious metals	150-200	Anode: $H_2+2OH^-=H_2O+2e^-$ Cathode : $1/2O_2+H_2O+2e^-=2OH^-$
Direct methanol	Proton exchange membrane	Pt- Ru on anode, Pt on cathode	30- 80	Anode : $CH_3OH+H_2O=CO_2+6H^+$ Cathode:$3/2O_2+6H^+ +6e^-=3H_2O$
Phosphoric acid	Phosphoric acid	Pt on anode and cathode	180-200	Anode: $H_2=2H^++2e^-$ Cathode: $1/2O_2+2H^++2e^-$=H2O
Molten carbonate	Lithium / Potassium Carbonate	Non-precious metals	650	Anode: $H_2+CO_3^{2-}$ $=H_2O+CO_2+2e^-$ Cathode: $1/2O_2+CO_2+2e^-=CO_3^{2-}$
Solid oxide	Yittria stablized Zirconia	Nickel on anode and perovskite oxide on cathode	1000	Anode: $H_2+O_2-=H_2O+2e^-$ Cathode: $1/2O_2+2e^-=O^{2-}$

1.2.1 Proton exchange membrane fuel cell (PEMFC)

Another type of fuel cell which use hydrogen as fuel, oxygen as oxidant and polymer membrane as electrolyte is called PEMFC being developed for transportation, stationary fuel cell, and portable fuel cell application. The component of PEMFC consists of anode and cathode as electrodes and polymer membrane is between anode and cathode electrodes which should be well ion conductor. Moreover, polymer membrane can protect the directly mixing of hydrogen and oxygen in PEMFC. The components and flow directions of PEMFC is shown in Fig. 1.2.

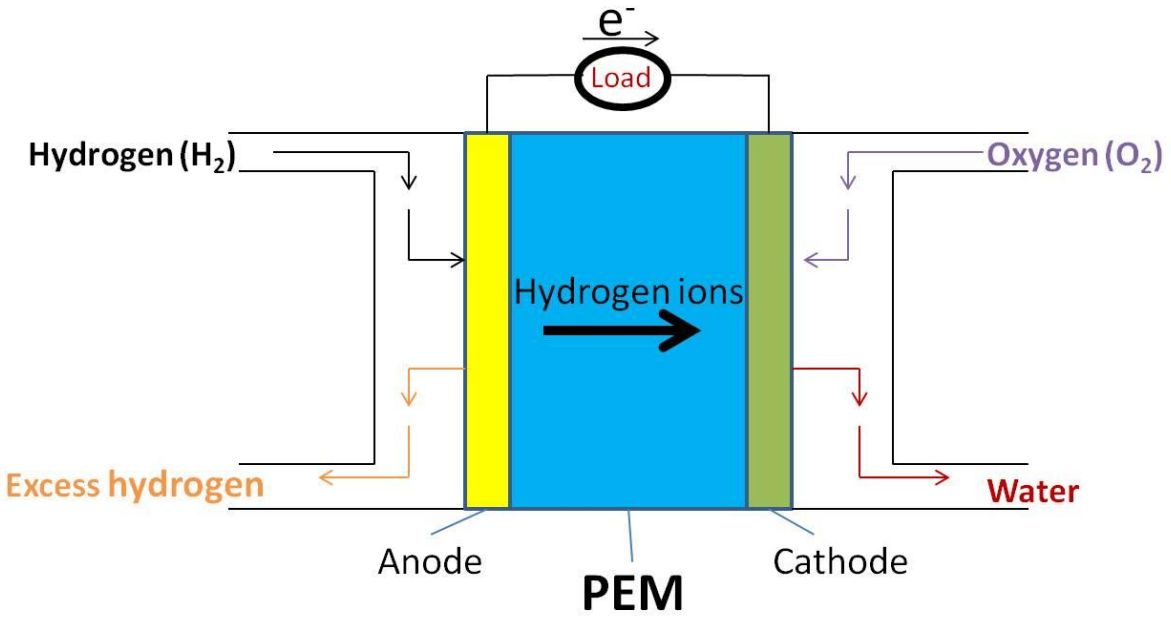

Fig. 1.2 Components and flow directions of a Proton Exchange Membrane Fuel Cell.

There are two reactions during operation;

- Hydrogen oxidation reaction at anode

$$H_2\,(g) \Leftrightarrow 2H^+ + 2e^- \qquad E=0.0\text{V vs RHE} \quad (1)$$

- Oxygen reduction reaction at cathode

$$O_2 + 4H^+ + 4e^- \Leftrightarrow 2H_2O \qquad E=1.23\text{V vs RHE} \quad (2)$$

The phenomena of PEMFC operation are complex which described in reference [8,9]. All components have effect to the performance of PEMFC. These phenomena occur in various components, need to research to improve performance of PEMFC such as membrane [10-14], gas diffusion layer [15-20], gas flow channels [21-27], and catalyst. In this study, we focus to improve durability of Pt-based catalyst for PEMFC application.

1.2.2 Oxygen reduction reaction (ORR) specific for PEMFC

The ORR has a complicated mechanism and sluggish kinetics that occurs at the cathode [28,29]. Due to the complicated mechanism and sluggish kinetics of the ORR, a higher amount of Pt is required for several times at the cathode electrode compared at anode electrode [30]. ORR in acidic electrolyte can occur into two routes [31]. The preferred dissociative route is a process of direct water formation from hydrogen and oxygen with four electron transfer. Active oxygen atoms (O*) were broken from the O=O bond which adsorbed on metal catalyst surface from O_2. The equation of this mechanism is written following as below:

$$1/2\ O_2 + * \rightarrow O* \tag{3}$$

These single active oxygen atoms are protonated by hydrogen ion (H^+) from anode electrode across polymer electrolyte membrane and reduced by electrons to produce hydroxyl groups (OH*) on metal catalyst surface[32]. The equation of this mechanism is written following as below:

$$O* + H^+ + e^- \rightarrow OH* \tag{4}$$

And then water is produced from reduction and protonation of OH* and finally, the water leaves from the metal catalyst surface. The equation of this mechanism is written following as below:

$$OH* + H^+ + e^- \rightarrow H_2O + * \tag{5}$$

Another route, when O_2 adsorbed on catalyst surface but no breaking of O=O bond and then O_2 changed form to HO_2* by reduction and protonation of O_2* which shown in Equations (6) and (7) [33]. This route is observed to produce H_2O_2 which is two electron transfer process. Since unclear

mechanisms of H_2O_2 formation, the possible mechanisms are proposed in Equation (8) and (9) [33].This route is called associative route.

$$O_2 + * \rightarrow O_2* \quad (6)$$

$$O_2* + H^+ + e^- \rightarrow HO_2* \quad (7)$$

$$HO_2* + H^+ + e^- \rightarrow H_2O_2* \quad (8)$$

$$H_2O_2* \rightarrow H_2O_2 + * \quad (9)$$

The possible dissociative and associative ORR mechanisms at cathode electrode are shown in Fig 1.3. Formation of H_2O_2 is highly undesirable in a PEMFC which H_2O_2 can diffuse into the polymer membrane and affects to performance of polymer membrane since polymer membrane is degraded [34]. In the ORR, H_2O_2 should not occur in during operation whereas poor catalyst produces significant amounts of H_2O_2 through associative route of ORR [35]. Due to much corrosive environment in acidic electrolyte at cathode electrode, the ORR catalyst must be stable. Moreover, binding energy of each metal catalyst is concerned for ORR. So, the ORR catalyst is essential and important to study for PEMFC.

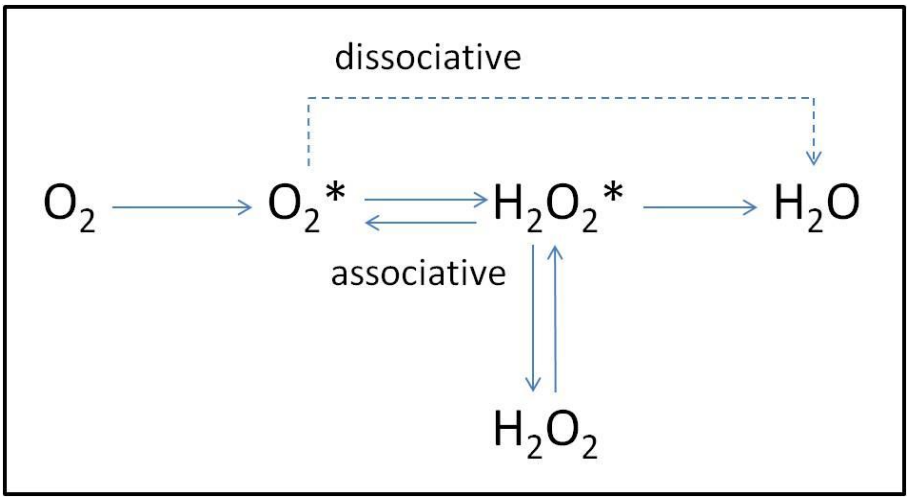

Fig. 1.3 Schematic of possible dissociative and associative mechanisms of ORR at cathode.

1.3 Challenges of ORR catalyst for PEMFC

1.3.1 Platinum-based catalysts

The key point of the performance of PEMFC is catalytic activity and durability of catalyst in oxygen reduction reaction at cathode electrode of PEMFC. The binding energy of metal catalyst is much concerned for ORR since it affects to the adsorption of O_2 on metal catalyst surface and product releasing from metal catalyst surface. If the binding energy is too high, the product (H_2O) could not well release from metal catalyst surface which H_2O will restrict the continuous reaction. If the binding energy is too low, the adsorption of O_2 on metal catalyst surface is not well which affects to slowly reaction or no reaction occur.

Low catalytic activity of ORR is cause of too high or too low binding energy between O_2 and metal catalyst, the diagram plot between oxygen reduction activity and oxygen binding energy was reported by J. K. Nørskov *et al.* [33]. It is observed that Pt shows the best activity, although the O_2 binding energy was about 0.2 eV which is too high [36]. Metals such as copper (Cu), nickel (Ni) and Iron (Fe), the O_2 binding oxygen of these metals are too high which affects to the removal of O and OH species on metal surface. For this reason, catalyst surface becomes to be unreactive surface since the catalyst surface was easily oxidized. In case of silver (Ag) and gold (Au), the O_2 binding energy is too low and the catalytic activity rate is limited for these metals since the transfer of hydrogen ion and electrons to oxygen atom on metal surface is not quite well [34].

The binding of O and followed by OH on catalyst surface is greatly necessary for ORR mechanism which is written in Equation (4) and (5), respectively. It is not only oxygen binding energy that determines the activity of a surface for oxygen reduction but the OH binding energy is also important. J. K. Nørskov *et al.* reported the diagram of both binding energies of O and OH against the activity [33]. From the diagram, we can see that the best metal catalyst for activity is Pt and both binding energies of O and OH of Pt are also best value for reactions. To enhance the catalytic activity of Pt-based catalyst, many researchers have studied about structure control for cathode electrode catalyst of PEMFC [37-48]. Pt is the best catalytic activity catalyst in nowadays. However, Pt catalysts suffer from limited durability under PEMFC operating conditions [49-53]. The Pt nanoparticles could be highly degraded in acidic electrolyte conditions [54-56]. The Pt nanoparticles might dissolved in acidic electrolyte or detach from carbon supports at cathode

electrode. Pt nanoparticles can also grow to undesired large particles which affect to the decreasing of active area to react between catalyst, fuel and oxidant by both agglomeration of Pt nanoparticles and Ostwald ripening phenomena [57-60].

1.3.2 Non-noble metal-based catalysts

Due to the Pt is rare element and cost of Pt catalyst is quite high which are problems to produce in commercially production, research towards to study others catalyst instead of Pt catalyst as non-noble metal-based catalysts to be candidate catalysts for the oxygen reduction reaction at cathode electrode in PEMFC. At the cathode electrode Pt typically contains 80-90 % of the total Pt in the PEMFC [61,62]. Therefore, the development of non-noble metal-based catalyst is largely focused to be alternative catalyst instead of Pt. There are many types of non-noble metal-based catalyst such as composite catalysts between transition metal and nitrogen doped carbon (M/N-doped C), with M refers to transition metal such as Fe or Co [50,61,63-70], transition metal oxides, nitrides and/or carbides [71-75] and transition metal chalcogenides [76-80]. Hye Ryung Byon *et al*. has studied the preparation of two composites catalyst which the first one produced from iron salt and graphitic carbon nitride and another one produced from iron salt and reduced graphene. The heat treatment is used to be synthesis method in this study. The results showed that the composite catalyst which produced from iron salt and reduced grapheme had higher activity in an acidic electrolyte compare with the composite catalyst which produced from iron salt and graphitic carbon nitride. The ORR activity was decreased to ~45% of the initial value during the stability test [81]. Composite catalyst between Co and nitrogen doped graphene was investigated by Kexing Niu *et al.*, in this study the media electrolyte is basic electrolyte. The catalyst (Co/N/rGO(NH_3)) which prepared in this experiment had similar ORR activity compare with Pt/C(20%) . After 20,000 s of durability test, the current of Co/N/rGO(NH_3) still remains 86.5%. In case of Pt/C (20%), the current remains approximately 73.3% after 20,000 s [82]. Although, non-noble metal-based catalyst shows high catalytic activity and durability in a basic media electrolyte but in case of an acidic media electrolyte the catalyst still have poor catalytic activity and durability compared with Pt-based catalyst [83,84].

1.3.3 Non-metal based catalysts

The fast and stable catalytic reaction of oxygen reduction reaction (ORR) is limited by the catalyst at the cathode electrode in PEMFC which are well known that the Pt-based catalysts showed well performance. However, their high cost and poor durability is mainly cause of restriction for large-scale commercialization. Recently, non-noble metal-based catalysts has been considered one of the most active and competitive catalyst to develop and study in order to replace the Pt-based catalysts for PEMFC. Especially, nitrogen-doped carbon nanotubes and graphene [85-92] have much interested since their properties including good durability, excellent electrocatalytic activities and low cost, which is alternative way to investigate for ORR catalysts. Zhi Yang *et al.* have studied the synthesis of carbon in sphere shape which doped with nitrogen. The reactants is sprayed and heated without air and catalyst. The relative current of NCS-H after 8000 s is approximately 94.26%, which is significantly higher than Pt/C catalyst (69.45%). From this result, it confirms that the carbon in sphere shape which doped with nitrogen in this study exhibits more stable than Pt/C catalyst in methanol and alkaline fuel cells [93].

Beside the carbon materials which doped with nitrogen, graphite materials also were studied in term of doping of phosphorous into graphite layers [94] including carbon nanotubes which doped with boron [95]. The aim in the study of doping single element in carbon materials is investigation of the enhancement of the catalytic activity for ORR. Carbon nanotubes which doped with boron is studied by Hu *et al.*. The results show that carbon nanotubes which doped with boron had good electrocatalytic activity for the ORR since onset potential shifted more close to the Pt catalyst's onset potential than without doping. With increasing boron content, electrocatalytic activity improved. From many researchers reported that single element doping on carbon materials enhance the catalytic activity of carbon materials for ORR. Two and multi elements doping on carbon materials were investigated [96-98] to improve the catalytic activity of single element doping on carbon materials. However, non-metal based catalysts still need more investigation to be candidate catalyst instead of Pt catalyst in the future [99].

1.4 Enhancement of durability for ORR catalyst

1.4.1 Platinum -based alloy catalyst

Many metal elements such as gold, cobalt and palladium are formed with platinum to be alloy metals have been widely studied in order to enhance the activity and durability of the Pt-catalysts at PEMFCs cathode electrode. Toda *et al.* investigated Pt alloys which were formed between nickel, cobalt, iron and platinum to determine electrocatalytic activity compared with pure Pt-catalysts. In case of Ni-Pt alloy was found that at content of Ni is approximately 30%, the activity exhibited maximum activity. Moreover, Co-Pt alloy which approximately 40% content of Co showed the maximum activity and the last Fe-Pt alloy was observed at approximately 50% content of Fe had maximum activity. B. Lim *et al.* found that the alloy between Pd and Pt which formed nanodendrites shape had higher activity than Pt/Cs about two and a half times base on the same amount of Pt. If the activity compared with Pt-black catalyst, the alloy between Pd and Pt which formed nanodendrites shape shows five times [100-103]. In case of Pt is formed to be alloy metal with non-noble transition metals such as cobalt, nickel, copper, chromium and iron, a large number of studies demonstrated to enhancement of the ORR activity as compared with Pt catalyst [104-111]. There are many researchers have studied PtCo bimetallic catalysts, where Pt:Co ratios of 1:1 to 3:1 are most studied during the last decade. The result showed that the catalytic activity of PtCo alloy exhibited higher than that of pure Pt [50,106,112,113]. PtNi bimetallic catalysts is investigated by Stamenkovic *et al.*, it was reported that the ORR activity for $Pt_3Ni(111)$ single crystal surfaces increase nearly two times over a commercial one [114,115]. In recent years, Strasser *et al*. have extensively investigated $PtCu_3$ alloys supported on carbon to enhance the ORR activity of Pt [30,114-119]. The $PtCu_3$ alloy catalysts exhibited a 4-6 fold higher specific activity than commercially Pt/C catalyst after voltammetric dealloying. Due to the dealloying of catalyst, the formation of a Pt-rich shell and Cu-rich core occurred which it is believed that cause of the superbly enhanced ORR activity of PtCu alloys [116, 120]. Adzic *et al.* have studied Pt-Au composite catalyst which synthesized with galvanic replacement method [121]. It was observed that the Pt-Au composite electrocatalyst can be stabilized against dissolution during 30,000 potential cycling. The current density of Au/Pt/C electrocatalyst after 30,000 cycles test is approximately higher 2.5 times than Pt/C catalyst.

However, the metal elements which formed with Pt to be alloy catalysts still dissolve in acidic electrolyte at the cathode electrode. The dissolution of the non-noble transition metal also

contributes to deactivation of the catalysts. The polymer electrolyte membrane could be deposited from the dissolved metal elements, which membranes will loss ability to transfer proton [122-127].

1.4.2 Surface coating

A high performance fuel cell catalyst needs long lifetime catalytic activity, no removal of catalyst from carbon materials, no migration of catalyst to membrane and no loss of the electrochemically active surface area (ECSA). All factor of desired catalyst is also an important for performance of fuel cell. The literature [3,128-132] reported and summarized the degradation mechanisms of Pt/C catalysts such as platinum dissolution, agglomeration of Pt, particles detachment that has been suggested to occur in PEMFC.

1.4.2.1 Conductive polymer coating

The conducting polymers such as polyaniline (PI), polypyrrole (PPY) and poly(3,4-ethylene-dioxythiophene) (PEDOT) are the interested materials for the ORR since their properties such as mechanical, , chemical, optical and electronic [133]. S. Chen *et al.* [134] studied the synthesis conductive polymer coating on Pt/C which aniline was used as conductive polymer source. In this study, the catalyst is formed to core-shell structure which conductive polymer, polyaniline (PANI), covered on Pt/C. The thicknesses of PANI shell depend on the loading of PANI which the thickness of 5 nm of PANI shell (30% loading of PANI) show highest the catalytic activity. After 1,500 cycles of CV measurement, the catalyst with 30% loading of PANI enhance the durability approximately 3 times compared to Pt/C. Carbon/poly(3,4-ethylene dioxythiophene) (C/PEDOT) composites are synthesized by in situ chemical oxidative polymerization of EDOT monomer on carbon black with different dopants including polystyrene sulfonic acid (PSSA), *p*-toluenesulfonic acid (*p*-TSA) and camphorsulfonic acid (CSA) with the addition of ethylene glycol (EG)or dimethyl sulfoxide (DMSO) are investigated by F. Memioğlu *et al*.. The results show that the composite prepared at 25 °C with *p*-TSA and EG exhibits the best carbon corrosion resistance. Pt/C/PEDOT: p-TSA was synthesized by using microwave irradiation technique also was investigated in this study, and it was seen that the prepared catalyst did not significantly lose oxygen reduction reaction activities after electrochemical oxidation [135].

Moreover, the metal-free catalyst for the ORR was developed with conducting polymer as the research of S. Wang *et al.*; nonaligned and vertically aligned CNT (CNT and ACNT, respectively) were modified with poly(diallyldimethylammonium chloride) (PDDA) by spin coating and infiltrating PDDA chains into the nanotube array, respectively. To investigate the ORR performance, Pt/C, bare CNT, bare ACNT and both conductive polymer-CNT and conductive polymer-ACNT and electrocatalysts were prepared on a rotating disk electrode (RDE) to measure by the linear sweep voltammetry (LSV) technique in alkaline solution (0.1 M KOH) which purged with O_2. The scan rate of potential and rotation rate of electrode are fixed at 10 mV s^{-1} and 1600 rpm, respectively. The ORR onset potential at the PDDA-CNT and PDDA-ACNT significantly shifted positively to -0.14 V and -0.09 V, respectively and the limiting diffusion current is approximately at -0.4 V. At -0.4 V of PDDA-ACNT had higher the ORR current density than PDDA-CNT and bare CNT by 1.5 and 4.5 times, respectively. Although the onset potential of ORR of PDDA-ACNT is lower than that of the Pt/C but there is no different in case of the limiting diffusion current density [136].

1.4.2.2 Silica coating

Novel strategy to prevent degradation mechanisms is silica coating, which silica is coated on catalyst to avoid agglomeration and prevent particles detachment; this alternative method is still not as widespread in the investigation. Recently, silica coated on Platinum/carbons was studied by Takenaka *et al*. to enhance the durability and activity of catalysts, the mechanisms of silica-coated Pt/C was proposed that the functionalized-carboxyl group carbon is binded by 3-aminopropyltriethoxysilane and then silica was generated with successive hydrolysis of Tetraethyl orthosilicate [137-140]. In these studies, the electrochemically active surface area of silica coated Platinum/carbons were higher than that of non-coated Platinum/carbons after durability test. The ORR activity of Platinum/carbons rapidly decreased during the durability test but in case of silica coated Platinum/carbons; the ORR activity was stable at all during the durability test. From these results show that the silica coated Platinum/carbons enhance the durability and the activity of catalyst is quite similar to that of non-coated catalyst. However, the preparation of catalyst needs to use toxic and strong acid (8M H_2SO_4 and 8M HNO_3) to modify carboxyl group on carbon surface due to the carboxyl group is a key for binding 3-aminopropyltriethoxysilane (APTES) on carbon surface [141]. To avoid dissolution of Pt from using strong acid, multiple processes are required in catalyst preparation.

In the present study, we aims to synthesize silica-coated Pt/C and Pt/CNT catalyst to enhance the durability for PEMFC in one step process without dissolving Pt catalyst by using three various type of surfactants (1) cationic surfactant (Cetyltrimethylammonium bromide (CTAB)), (2) anion surfactant (Sodium dodecylbezenesulfonate (SDBS)), and (3) non-ionic surfactant (Pluronic 123 (P123)) to induce and neucleate silica supported on Pt/C and benzoic acid in the pH range 2-4 to introduce carboxyl group on carbon surface and covered with silica layers to (1) avoid the agglomeration of the nanoparticles and (2) to prevent detachment from carbon supports. This study is expected to provide an alternative solution for high durability electrode material for PEMFCs.

1.5 Objective and outline of thesis

As mentioned earlier about the motivations and the problem of Pt-based catalyst for oxygen reduction reaction at cathode electrode of PEMFC. The aim of this thesis is to attain the following objectives:

> To enhance durability of Pt-based catalyst (commercial Pt/C) and Pt nanoparticles supported on carbon nanotubes by silica coating to avoid the agglomeration of the Pt nanoparticles and to prevent detachment of Pt nanoparticles from carbon supports with different surfactants and benzoic acid.

The thesis is organized into six chapters, describing the details of my scientific research and the experimental results as follows:

Chapter 1 presents a brief introduction of Fuel cell. An overview of types of fuel cell is then given. Additionally, the challenge of catalyst for oxygen reduction reaction at cathode electrode of PEMFC is introduced.

Chapter 2 silica coating synthesis diagram and experimental setup for Pt supported on carbon nanotubes synthesizing are given. The silica coating on commercial Pt supported on carbon and carbon nanotubes procedure are given in detail.

Chapter 3 describes and discusses the effect of different types of surfactant which use for synthesize silica-coated commercial Pt supported on carbon (Pt/C) to the enhancement of durability in during operation. The investigation of structural morphology and durability are presented.

Chapter 4 describes and discusses the enhancement of durability of silica-coated Pt supported on carbon nanotubes (Pt/CNT) which has difference structure from Pt/C compare to uncoated Pt/CNT.

Chapter 5 describes and discusses the effect of amount of benzoic acid which use in synthesizing silica-coated Pt/C to the enhancement of durability in an acidic electrolyte during operation where chapter 6 summarizes all the above chapters in the thesis.

References

[1] M. K. Debe, *Nature*, 2012, **486**, 43-51.

[2] "The Fuel Cell Industry Review 1012", *Fuel Cell Today*, Royston, Hertfordshire, UK, 2012.

[3] R. Borup, J. Meyers, B. Pivovar, Y. S. Kim, R. Mukundan, N. Garland, D. Myers, M. Wilson, F. Garzon, D. Wood, P. Zelenay, K. More, K. Stroh, T. Zawodinski, J. Boncella, J. E. McGrath, M. Inaba, K. Miyatake, M. Hori, K. Ota, Z. Ogumi, S. Miyata, A. Nishikata, Z. Siroma, Y. Uchimoto, K. Yasuda, K. Kimijima, and N. Iwashita, *Chem. Rev.* 2007, **107**, 3904–3951.

[4] J. C. Meier, C. Galeano, I. Katsounaros1, J. Witte, H. J. Bongard, A. A. Topalov, C. Baldizzone, S. Mezzavilla, F. Schüth, and K. J. J. Mayrhofer, *Beilstein J. Nanotechnol.* 2014**, 5**, 44–67.

[5] R. O'Hayre, S. K. Cha, W. Colella, F. B. Prinz, "Fuel Cell Fundamentals", New York, John Wiley & Sons, 2006.

[6] J. H. Hirschenhofer, D. B. Stauffer, R. R. Engleman, and M. G. Klett, "Fuel Cell Handbook, Forth Edition", Parsons Corporation, Reading, PA, 1998.

[7] L.J. Blomen, and M.N. Mugerwa, "Fuel Cell Systems", Plenum Press, New York, N.Y., 1993

[8] O. T. Holton, and J. W. Stevenson, Platinum Metals Rev., 2013, **57**, 259-271.

[9] Y. Wang, K. S. Chen, J. Mishler, S. C. Cho, and X. C. Adroher, *Applied Energy*, 2011, **88**, 981–1007.

[10] Y. L. Ma, J. S. Wainright, M. H. Litt, and R. F. Savinell, *J. Electrochem Soc*, 2004, **151**, A8–A16.

[11] J. Zhang, Z. Xie, J. Zhang, Y. Tang, C. Song, T. Navessin, Z. Shi, D. Song, H. Wang, D. P. Wilkinson, Z. S. Liu, and S. Holdcroft, *Journal of Power Sources*, 2006, **160**, 872–891.

[12] S. Atkinson, *Membrane Technol*, 2005, **1**, 5–7.

[13] A. A. Kornyshev, A. M. Kuznetsov, E. Spohr, and J. Ulstrup, *J. Phys. Chem. B*, 2003, **107**, 3351-3366.

[14] G. J. Elfring, and H. Struchtrup, *Journal of Membrane Science*, 2008, **315**, 125–132.

[15] T. R. Ralph, G. A. Hards, J. E. Keating, S. A. Campbell, D. P. Wilkinson, M. Davis, J. St-Pierre, and M. C. Johnson, *J. Electrochem. Soc.*, 1997, **144**, 11, 3845-3857.

[16] Y. Wang, C. Y. Wang, and K. S. Chen, *Electrochimica Acta*, 2007, **52**, 3965–3975.

[17] Y. Wang, S. Cho, R. Thiedmann, V. Schmidt, W. Lehnert, and X. Feng, *International Journal of Heat and Mass Transfer*, 2010, **53**, 1128–1138.

[18] V. P. Schulza, P. P. Mukherjeeb, J. Beckerc, A. Wiegmannc, and C. Y. Wang, *ECS Trans.*, 2006**,** 3, 1069-1075.

[19] P. K. Sinha, P. P. Mukherjee, and C. Y. Wang, *J. Mater. Chem.*, 2007, **17**, 3089-3103.

[20] P. P. Mukherjeea, C. Y. Wang, Q. Kang, *Electrochimica Acta*, 2009, **54**, 6861–6875.

[21] D. H. Jeon, S. Greenway, S. Shimpalee, and J.W. Van Zee, *Int J Hydrogen Energy*, 2008, **33**, 1052–1066.

[22] S. Karvonen, T. Hottinen, J. Saarinen, and O. Himanen, *Journal of Power Sources*, 2006, **161**, 876–884.

[23] S.-W Perng, H.-W. Wu, T.-C. Jue, and K. –C. Cheng, *Applied Energy*, 2009, **86**, 1541–1554.

[24] S.-W. Perng, and H.-W. Wu, *Applied Energy*, 2011, **88**, 52–67.

[25] G. Inoue, Y. Matsukuma, and M. Minemoto, *Journal of Power Sources*, 2006, **157**, 136–152.

[26] Y. Wang, *J. Electrochem Soc*., 2009, **156**, B1134–1141.

[27] X.-D. Wanga, Y.-Y. Duanb, W.-M. Yan, D.-J. Lee, A. Sue, and P.-H. Chi, *Journal of Power Sources*, 2009, **193**, 684–690.

[28] H. A. Gasteiger and N. M. Marković, *Science*, 2009, **324**, 48-49.

[29] F. T. Wagner, B. Lakshmanan and M. F. Mathias, *J. Phys. Chem. Lett.*, 2010, **1**, 2204-2219.

[30] A. J. Appleby, *J. Electroanal. Chem.*, 1993, **357,** 117-179.

[31] J. Zhang, "PEM Fuel Cell Electrocatalysts and Catalyst Layers: Fundamentals and Applications", Springer Verlag London Ltd, Guildford, Surrey, UK, 2008.

[32] R. Jinnouchi, *Microscale Thermophys. Eng.*, 2003, **7**, 15-31.

[33] J. K. Nørskov, J. Rossmeisl, A. Logadottir, L. Lindqvist, J. R. Kitchin, T. Bligaard and H. Jónsson, *J. Phys. Chem. B*, 2004, **108**, 17886-17892.

[34] R. Borup, J. Meyers, B. Pivovar, Y. S. Kim, R. Mukundan, N. Garland, D. Myers, M. Wilson, F. Garzon, D. Wood, P. Zelenay, K. More, K. Stroh, T. Zawodzinski, J. Boncella, J. E. McGrath, M. Inaba, K. Miyatake, M. Hori, K. Ota, Z. Ogumi, S. Miyata, A. Nishikata, Z. Siroma, Y. Uchimoto, K. Yasuda, K.-i. Kimijima and N. Iwashita, *Chem. Rev*., 2007, **107**, 3904-3951.

[35] K. S. Lyons, M. Teliska, W. Baker and J. Pietron, "Low Platinum Catalysts for Oxygen Reduction at PEMFC Cathodes", DOE Hydrogen Program, US Department of Energy, Washington, DC, USA, 2005.

[36] V. Stamenkovic, B. S. Mun, K. J. J. Mayrhofer, P. N. Ross, M. N. Markovic, J. Rossmeisl, J. Greeley and J. K. Nørskov, *Angew. Chem. Int. Ed*., 2006, **45**, 2897-2901.

[37] P. Strasser, S. Koha, and J. Greeley, *Phys. Chem. Chem. Phys.*, 2008, **10**, 3670-3683.

[38] R. Srivastava, P. Mani, N. Hahn, and P. Strasser, *Angew. Chem. Int. Ed.,* 2007, **46**, 8988 –8991.

[39] A. Sarkar, and A. Manthiram, *J. Phys. Chem. C*, 2010, **114**, 4725–4732.

[40] S. Koh, and P. Strasser, *J. Am. Chem. Soc.*, 2007, **129**, 12624–12625.

[41] V. R. Stamenkovic, B. Fowler, B. S. Mun, G. F. Wang, P. N. Ross, C. A. Lucas, and N. M. Markovic, *Science*, 2007, **315**, 493-497.

[42] V. Stamenkovic, B. S. Mun, K. J. J. Mayrhofer, P. N. Ross, N. M. Markovic, J. Rossmeisl, J. Greeley, and J. K. Norskov, *Angew. Chem. Int. Ed.*, 2006, **45**, 2897 –2901.

[43] V. Stamenkovic, T. J. Schmidt, P. N. Ross, N. M. Markovic, *J. Electroanal. Chem*., 2003, **554-555**, 191-199.

[44] M. K. Debe, A. K. Schmoeckel, G. D. Vernstrorn, and R. Atanasoski, *J. Power Sources* , 2006, **161**, 1002-1011.

[45] R. R. Adzic, J. Zhang, K. Sasaki, M. B. Vukmirovic, M. Shao, J. X. Wang, A. U. Nilekar, M. Mavrikakis, J. A. Valerio, and F. Uribe, *Top Catal.*, 2007, **46**, 249-262.

[46] K. Sasaki, Y. Mo, J. X. Wang, M. Balasubramanian, F. Uribe, J. Mcbreen, and R. R. Adzic, *Electrochim. Acta*, 2003, **48**, 3841-3849.

[47] M. B. Vukmirovic, J. Zhang, K. Sasaki, A. U. Nilekar, F. Uribe, M. Mavrikakis, and R. R. Adzic, *Electrochim. Acta*, 2007, **52**, 2257-2263.

[48] V. Stamenkovic, T. J. Schmidt, P. N. Ross, and N. M. Markovic, *J. Phys. Chem. B*, 2002, **106**, 11970-11979.

[49] F. A. de Bruijn, V. A. T. Dam, and G. J. M. Janssen, *FUEL CELLS*, 2008, **8**, 3–22.

[50] H. A. Gasteiger, S. S. Kocha, B. Sompalli, and F. T. Wagner, *Applied Catalysis B: Environmental*, 2005, **56**, 9-35.

[51] W. Vielstich, A. Lamm, and H. A. Gasteiger, Handbook of Fuel Cells, Fundamentals Technology and Applications, 2003.

[52] S. S. Zhang, X. Z. Yuan, J. N. C. Hin, H. J. Wang, K. A. Friedrich, and M. Schulze, *Journal of Power Sources*, 2009, **194**, 588-600.

[53] J. Willsau, J. Heitbaum, *J. Electroanal. Chem*., 1984, 1**61**, 93-101.

[54] A. Honji, T. Mori, K. Tamura, Y. Hishimura, *J. Electrochem. Soc*., 1988, **135**, 355-359.

[55] A. C. C. Tseung, S. C. Dhara, *Electrochimica Acta*, 1975, **20**, 681-683.

[56] G. A. Gruver, R. F. Pascoe, H. R. Kunz, *J. Electrochem. Soc*., 1980, **127**, 1219-1224.

[57] S. Mukerjee, and J. Mcbreen, *J. Electroanal. Chem*., 1998, **448**, 163-171.

[58] M. K. Min, J. H. Cho, K. W. Cho, and H. Kim, *Electrochim. Acta*, 2000, **45,** 4211-4217.

[59] S. Chen, H. A. Gasteiger, K. Hayakawa, T. Tada, and Y. Shao-Horn, *J. Electrochem. Soc*., 2010, **157**, A82-A97.

[60] S. C. Ball, S. L. Hudson, D. Thompsett, and B. Theobald, *J. Power Sources*, 2007, **171**, 18-25.

[61] F. Jaouen, E. Proietti, M. Lefevre, R. Chenitz, J.-P. Dodelet, G. Wu, H. T. Chung, C. M. Johnston and P. Zelenay, *Energy Environ. Sci.*, 2011, **4**, 114-130.

[62] F. Barbir, PEM Fuel Cells: Theory and Practice, Elsevier Academic Press, 2005.

[63] A. A. Gewirth and M. S. Thorum, *Inorg. Chem.*, 2010, **49**, 3557-3566.

[64] C. W. B. Bezerra, L. Zhang, K. Lee, H. Liu, A. L. B. Marques, E. P. Marques, H. Wang and J. Zhang, *Electrochim. Acta*, 2008, **53**, 4937-4951.

[65] M. Lefevre, E. Proietti, F. Jaouen and J.-P. Dodelet, *Science*, 2009, **324**, 71-74.

[66] H. T. Chung, C. M. Johnston, K. Artyushkova, M. Ferrandon, D. J. Myers and P. Zelenay, *Electrochem. Commun*., 2010, **12**, 1792-1795.

[67] F. J. E. Proietti, M. Lefevre, N. Larouche, J. Tian, J. Herranz, and J.-P Dodelet, *Nat. Commun*., 2011, **2**.

[68] M. Kobayashi, H. Niwa, M. Saito, Y. Harada, M. Oshima, H. Ofuchi, K. Terakura, T. Ikeda, Y. Koshigoe, J. Ozaki and S. Miyata, *Electrochim. Acta*, 2012, **74**, 254-259.

[69] A. H. C. Sirk, S. A. Campbell and V. I. Birss, *J. Electrochem. Soc*., 2008, **155**, B592-B601.

[70] S. Gharaibeh, V. Birss, *ECS Trans.*, 2013, **58**, 1701-1712.

[71] Y. Liu, A. Ishihara, S. Mitsushima, N. Kamiya and K.-I. Ota, *J. Electrochem. Soc.*, 2007, **154**, B664-B669.

[72] J. Y. Kim, T.-K. Oh, Y. Shin, J. Bonnett and K. S. Weil, *Int. J. Hydrog. Energy*, 2011, **36**, 4557-4564.

[73] J.-H. Kim, A. Ishihara, S. Mitsushima, N. Kamiya and K.-I. Ota, *Electrochim. Acta*, 2007, **52**, 2492-2497.

[74] K. Lee, A. Ishihara, S. Mitsushima, N. Kamiya and K.-I. Ota, *Electrochim. Acta*, 2004, **49**, 3479-3485.

[75] H. Zhong, H. Zhang, G. Liu, Y. Liang, J. Hu and B. Yi, *Electrochem. Commun.*, 2006, **8**, 707-712.

[76] H. Behret, H. Binder and G. Sandstede, *Electrochim. Acta*, 1975, **20**, 111-117.

[77] D. Susac, L. Zhu, M. Teo, A. Sode, K. C. Wong, P. C. Wong, R. R. Parsons, D. Bizzotto, K. A. R. Mitchell and S.A. Campbell, *J. Phys. Chem. C*, 2007, **111**, 18715-18723.

[78] E. Vayner, R. A. Sidik, A. B. Anderson and B. N. Popov, *J. Phys. Chem. C*, 2007, **111**, 10508-10513.

[79] Y. Feng, T. He and N. Alonso-Vante, *Chem. Mater*., 2007, **20**, 26-28.

[80] K. Lee, L. Zhang and J. Zhang, *Electrochem. Commun*., 2007, **9**, 1704-1708.

[81] H. R. Byon, J. Suntivich and Y. Shao-Horn, *Chem. Mater*., 2011, **23**, 3421–3428.

[82] K. Niu, B. Yang, J. Cui, J. Jin, X. Fu, Q. Zhao and J. Zhang, *J. Power Sources*, 2013, **243**, 65-71.

[83] M. Lefevre, J. P. Dodelet, and P. Bertrand, *J. Phys. Chem. B*, 2002, **106**, 8705-8713.

[84] S. Gupta, D. Tryk, I. Bae, W. Aldred, and E. Yeager, *Journal of Applied Electrochemistry*, 1989, **19**, 19-27.

[85] K. P. Gong, F. Du, Z. H. Xia, M. Durstock and L. M. Dai, *Science*, 2009, **323**, 760-763.

[86] W. Xiong, F. Du, Y. Liu, A. Perez, M. Supp, T. S. Ramakrishnan, L. M. Dai and L. Jiang, *J. Am. Chem. Soc*., 2010, **132,** 15839-15841.

[87] T.C. Nagaiah, S. Kundu, M. Bron, M. Muhler, W. Schuhmann, *Electrochem. Commun*., 2010, **12**, 338-341.

[88] Y. F. Tang, B. L. Allen, D. R. Kauffman and A. Star, *J. Am. Chem. Soc*., 2009, **131**, 13200-13201.

[89] R. L. Liu, D. Q. Wu, X. L. Feng and K. Mullen, *Angew. Chem. Int. Ed*., 2010, **49**, 2565-2569.

[90] L. T. Qu, Y. Liu, J. B. Baek and L. M. Dai, *ACS Nano.*, 2010, **4**, 1321-1326.

[91] W. Yang, T. P. Fellinger and M. J. Antonietti, *J. Am. Chem. Soc.*, 2011, **133**, 206-209.

[92] D. S. Yu and L. M. Dai, *J. Phys, Chem. Lett*., 2010, **1**, 467-470.

[93] X. M. Zhou, Z. Yang, H. G. Nie, Z. Yao, L. J. Zhang and S. M. Huang, *J. Power Sources*, 2011, **196**, 9970-9974.

[94] Z. W. Liu, F. Peng, H. J. Wang, H. Yu, W. X. Zheng and J. Yang, *Angew. Chem. Int. Ed*., 2011, **50**, 3257-3261.

[95] L. Yang, S. J. Jiang, Y. Yu, L. Zhu, S. Chen, X. Z. Wang, Q. Wu, J. Ma, Y. W. Ma and Z. Hu, *Angew. Chem. Int. Ed.*, 2011, **50**, 7132-.

[96] S. Y. Wang, E. Iyyamperumal, A. Roy, Y. H. Xue, D. S. Yu and L.M. Dai, *Angew. Chem. Int. Ed.*, 2011, **50**, 11756-11760.

[97] S. Y. Wang, L. P. Zhang, Z. H. Xia, A. Roy, D. W. Chang, J .B. Baek and L. M. Dai, *Angew. Chem. Int. Ed*., 2012, **51**, 4209-4212.

[98] C. H. Choi, S. H. Park and S. I. Woo, *J. Mater. Chem*. 2012, **22**, 12107-12115.

[99] Z. Yang, H. Nie, X. Chen, X. Chen and S. Huang, *J. Power Sources*, 2013, **236**, 238-249.

[100] T. Toda, H. Igarashi, H. Uchida and M. Watanabe, *J. Electrochem. Soc*., 1999, **146**, 3750-3756.

[101] V. R. Stamenkovic, B. S. Mum, M. Arenz, K. J. J. Mayrhofer, C. A. Lucas, G. Wang, P. N. Ross, N. M. Markovic, *Nat. Mater*., 2007, **6**, 241-247.

[102] S. Takenaka, A. Hirata, E. Tanabe, H. Matsune, M. Kishida, *J. Catal*., 2010, **274**, 228-238.

[103] B. Lim, M. Jiang, P. H. Camargo, E. C. Cho, J. Tao, X. Lu, Y. Zhu, Y. Xia, *Science*, 2009, **324**, 1302-1305.

[104] P. Mani, R. Srivastava, and P. Strasser, *J. Power Sources*, 2011, **196**, 666-673.

[105] S. Mukerjee and S. Srinivasan, *J. Electroanal. Chem.*, 1993, **357**, 201-224.

[106] U. A. Paulus, A. Wokaun, G. G. Scherer, T. J. Schmidt, V. Stamenkovic, V. Radmilovic, N. M. Markovic and P. N. Ross, *J. Phys. Chem. B*, 2002, **106**, 4181-4191.

[107] V. Jalan and E. J. Taylor, *J. Electrochem. Soc.*, 1983, **130**, 2299-2302.

[108] B. C. Beard, and P. N. Ross, *J. Electrochem. Soc.*, 1990, **137**, 3368-3374.

[109] S. Chen, P. J. Ferreira, W. C. Sheng, N. Yabuuchi, L. F. Allard and Y. Shao-Horn, *J. Am. Chem. Soc.*, 2008, **130**, 13818-13819.

[110] I. Dutta, M. K. Carpenter, M. P. Balogh, J. M. Ziegelbauer, T. E. Moylan, M. H. Atwan and N. P. Irish, *J. Phys. Chem. C*, 2010, **114**, 16309–16320.

[111] K. Jayasayee, V. A. Dam, T. Verhoeven, S. Celebi and F. A. de Bruijn, *J. Phys. Chem. C*, 2009, **113**, 20371–20380.

[112] U. A. Paulus, A. Wokaun, G. G. Scherer, T. J. Schmidt, V. Stamenkovic, N. M. Markovic and P. N. Ross, *Electrochimica Acta*, 2002, **47**, 3787-3798.

[113] N. Travitsky, T. Ripenbein, D. Golodnitsky, Y. Rosenberg, L. Burshtein and E. Peled, *J. Power Sources*, 2006, **161**, 782-789.

[114] M. Wakisaka, S. Mitsui, Y. Hirose, K. Kawashima, H. Uchida and M. Watanabe, *J. Phys. Chem. B*, 2006, **110**, 23489-23496.

[115] K. Kinoshita, Electrochemical oxygen technology, Wiley, New York, 1992.

[116] S. Koh and P. Strasser, *J. Am. Chem. Soc.*, 2007, **129,** 12624-12625.

[117] R. Z. Yang, J. Leisch, P. Strasser and M. F. Toney, *Chem. Mater*., 2010, **22**, 4712–4720.

[118] P. Strasser, *Reviews in Chemical Engineering*, 2009, **25**, 255-295.

[119] P. Mani, R. Srivastava and P. Strasser, *J. Phys. Chem. C*, 2008, **112**, 2770-2778.

[120] P. Strasser, S. Koh, T. Anniyev, J. Greeley, K. More, C. F. Yu, Z. C. Liu, S. Kaya, D. Nordlund, H. Ogasawara, M. F. Toney and A. Nilsson, *Nat. Chem.*, 2010, **2**, 454-460.

[121] J. Zhang, K. Sasaki, E. Sutter and R. R. Adzic, *Science*, 2007, **315**, 220-222.

[122] T. Kunimoto, M. Inaba, Y. Nakayama, K. Ogata, R. Umebayashi, A. Tasaka, Y. Iriyama, T. Abe and Z. Ogumi, *J. Power Sources*, 2006, **158**, 1222−1228.

[123] E. Guilminot, A. Corcella, F. Charlot, F. Maillard and M. Chatenet, *J. Electrochem. Soc*., 2007, **154**, B96−B105.

[124] T. Okada, Y. Ayata, H. Satou, M. Yuasa, and I. Sekine, *J. Phys. Chem. B*, 2001, **105**, 6980−6986.

[125] S. C. Ball, S. L. Hudson, B. Theobald and D. Thompsett, *ECS Transactions*, 2007, **11**, 1267-1278.

[126] H. R. Colon-Mercado, H. Kim and B. N. Popov, *Electrochemistry Communications*, 2004, **6**, 795-799.

[127] H. R. Colon-Mercado and B. N. Popov, *J. Power Sources*, 2006, **155**, 253-263.

[128] Y. Shao-Horn, W. C. Sheng , S. Chen, P. J. Ferreira, E. F. Holby and D. Morgan, *Top Catal.*, 2007, **46**, 285–305.

[129] J. C. Meier, C. Galeano, I. Katsounaros, A. A. Topalov, A. Kostka, F. Schüth and K. J. J. Mayrhofer,

[130] J. C. Meier, I. Katsounaros, C. Galeano, H. J. Bongard, A. A. Topalov, A. Kostka, A. Karschin, F. Schüthb and K. J. J. Mayrhofer, *Energy Environ. Sci.*, 2012, **5**, 9319-9330.

[131] A. Zanaa, J. Spedera, M. Roefzaada, L. Altmannb, M. Bäumerb and M. Arenza, *J. Electrochem. Soc*.**,** 2013, **160**, F608-F615.

[132] F. R. Nikkuni, E. A. Ticianelli, L. Dubau and M. Chatenet, *Electrocatalysis*, 2013, **4**, 104–116.

[133] Rajesha, T. Ahuja, and D. Kumar, *Sens. Actuators B*, 2009, **136**, 275-286.

[134] S. Chen, Z. Wei, X. Qi, L. Dong, Y.-G. Guo, L. Wan, Z. Shao and L. Li, *J. Am. Chem. Soc.*, 2012, **134**, 13252−13255**.**

[135] F. Memioğlu1, A. Bayrakçeken, T. Öznülüer and M. Ak, *Int. J. Energy Res.*, 2014, **38**, 1278–1287.

[136] S. Wang, D. Yu and L. Dai, *J. Am. Chem. Soc.*, 2011, **133**, 5182–5185.

[137] S. Takenaka, T. Miyazaki, H. Matsune and M. Kishida, *Catal. Sci. Technol*., 2015, **5**, 1133-1142.

[138] S. Takenaka, H. Matsumori, K. Nakagawa, H. Matsune, E. Tanabe and M. Kishida, , *J. Phys. Chem. C*, 2007, **111**, 15133-15136.

[139] S. Takenaka, H. Matsumori, H. Matsune, M. Kishida, *Appl. Catal., A*, 2011, **409–410**, 248–256.

[140] S. Takenaka, H. Miyamoto, Y. Utsunomiya, H. Matsune and M. Kishida, *J. Phys. Chem. C*, 2014, **118**, 774-783.

[141] X. Li, W. Chen, Q. Zhan and L. Dai, *J. Phys. Chem. B*, 2006, **110**, 12621-12625.

Chapter 2

~ Experimental setups and characterization ~

~ Experimental setups and characterization ~

2.1 Silica coating synthesis diagram

2.1.1 Novel Silica-coating by sol-gel method

In this study, silica-coated on Pt/C and Pt/CNT synthesis is very simple. We applied the method from silica or mesoporous silica synthesis (sol-gel method). Diagram of silica coating synthesis for experiment in chapter 3 and 4 is shown in Fig. 2-1. In this experiment, Tetraethyl orthosilicate (TEOS) is used as silica precursor, sodium hydroxide is used to adjust pH of solution during synthesis, three types of surfactant (Cetyltrimethylamonium bromide (CTAB), Sodium dodecylbenzenesulfonate (SDBS), Pluronic P123 (P123)) are used to disperse and induce the silica precursor to nucleate and grow on Pt/C, and ethanol is used be as solvent in this synthesizing.

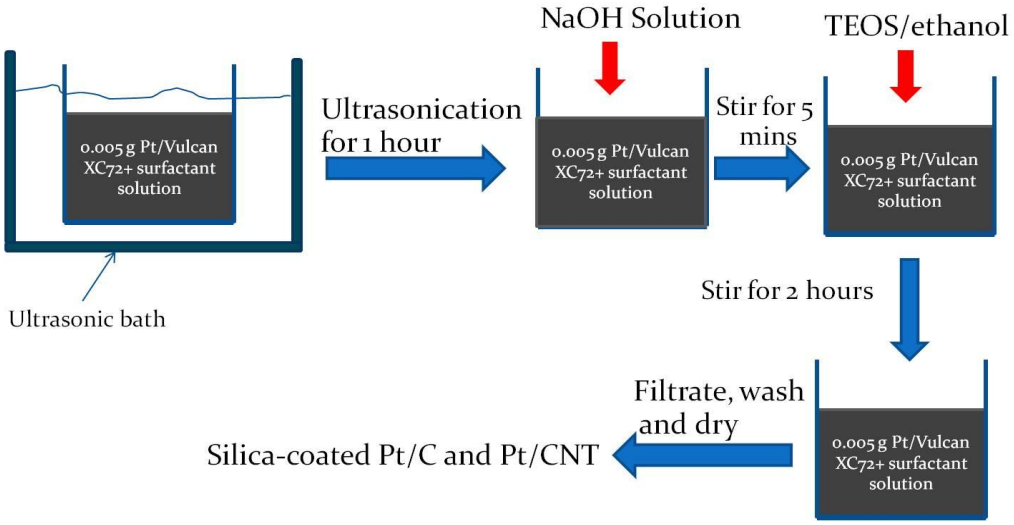

Figure 2.1 Silica coating synthesis diagram for experiment in chapter 3 and 4.

The procedures of this experiment are followed as below;

- Pt/C and Pt/CNT are dispersed in surfactant solution by sonicator for 1 hour.
- Adjust pH (~10) by adding NaOH solution in surfactant solution and then stir for 5 minutes.
- The mixture of TEOS and ethanol is injected to solution and then continue stir until 2 hours.

- The solution was filtrated and washed with pure water many times and dried at 80°C for 6 hours.
- Finally, solid sample was collected from filter paper and characterized.

2.1.2 Silica-coating by APTES and TEOS

For the experiment in chapter 5, Tetraethyl orthosilicate (TEOS) and 3-aminopropyltriethoxysilane (APTES) are used as silica precursor, benzoic acid is used to disperse and induce the silica precursor to nucleate and grow on Pt/C, and ethanol is used be as solvent in this synthesizing. The diagram of silica coating synthesis is show in Fig. 2-2

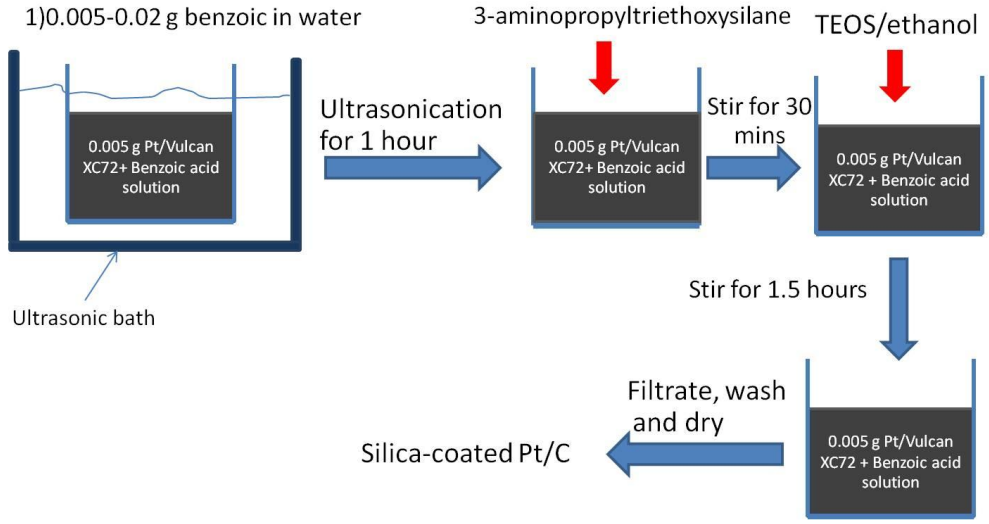

Figure 2.2 Silica coating synthesis diagram for experiment in chapter 5.

The procedures of this experiment are followed as below;

- Pt/C is dispersed in benzoic acid solution by sonicator for 1 hour.
- The mixture of APTES and ethanol is added in the solution and then stir for 30 minutes.
- After that the mixture of TEOS and ethanol is injected to solution and then continue stir for 1.5 hours.
- The solution was filtrated and washed with pure water many times and dried at 80°C for 6 hours.
- Finally, solid sample was collected from filter paper and characterized.
-

2.2 Pt supported on carbon nanotubes synthesis

2.2.1 Solution plasma process (SPP)

In this study, Pt/CNT were synthesized by solution plasma process (SPP). SPP is applied widely for metal nanoparticle synthesis nowadays. The details of SPP, including its mechanism and physical and chemical aspects have been published by the co authors [1-4]. The experimental set up is shown in Fig. 2.3. The system consisted of a pair of platinum electrodes (diameter of 1#mm, 99.95%, Nilaco, Japan) placed in a glass vessel (100 ml) and discharged in CNT suspension (0.01g of CNTs in distilled water) for 5, 10, and 15 min. The samples were labeled 5-Pt/CNTs, 10-Pt/CNTs, and 15-Pt/CNTs, respectively.The electrodes were connected to a bipolar–DC pulse power supply for plasma generation. The electrodes were insulated with ceramic tubes. The primary voltage, pulse frequency, pulse width, and electrode distance were fixed at 100 V, 20 kHz, 0.5 μs, and 0.5 mm, respectively.

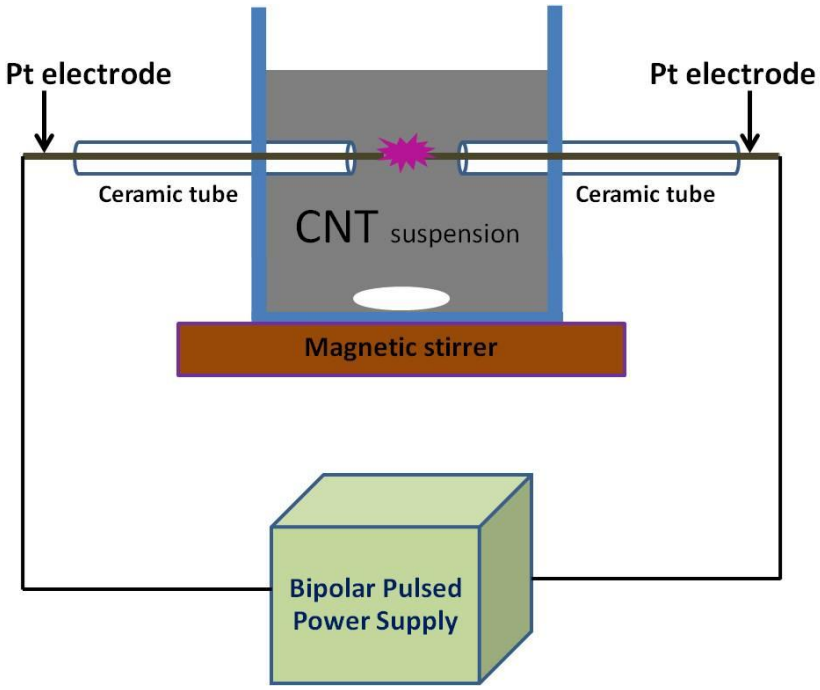

Figure 2.3 Experiment setup of Pt/CNT synthesis.

2.3 Characterizations of silica coated Pt carbon materials

2.3.1 Morphologies by transmission electron microscopy (TEM)

The morphology of Pt/C, Pt/CNTs, silica coated Pt/C and silica coated Pt/CNTs was observed through the transmission electron microscopy (TEM), JEM-2500SE. TEM was operated by the accelerating voltage of 200 kV. Further, the initial catalyst powders were sonicated in ethanol. A solution was pipette on Cu TEM grid and dried in air. After the electrochemical testing the catalyst was collected from glassy carbon electrode and sonicated in ethanol and then the solution was dropped on Cu TEM grid to characterize. The chemical composition of Pt-based catalysts before and after silica coating process was determined using an energy dispersive X-ray spectroscopy (EDS).

2.3.2 X-ray diffraction (XRD)

The structural properties of Pt/CNTS were examined using an X-ray diffractrometer (Rigaku SmartLab) with Cu Kα radiation (λ = 0.15418 nm) operating at 9 kW (45 mA, 200 V). 2θ range was used from 5° to 90°, the catalyst powder surface in holder should carefully flattened and flushed to form a smooth surface.

2.4 Electrochemical Analyses

2.4.1 Cyclic voltammetry (CV) measurement

Voltammetry is necessary method to analyze the electrocatalytic of electrocatalyst to evaluate the catalytic activity and the durability of electrocatalyst in fuel cell field. Especially the oxidation and the reduction reaction of catalyst in acidic and basic media electrolytes including mechanisms of electron transfer of catalyst studies [5]. The current and the voltage have relation during operation time. The voltage is swept with fixed rate from V_1 to V_2 and then is swept back to V_1 as shown in Figure 2.4.

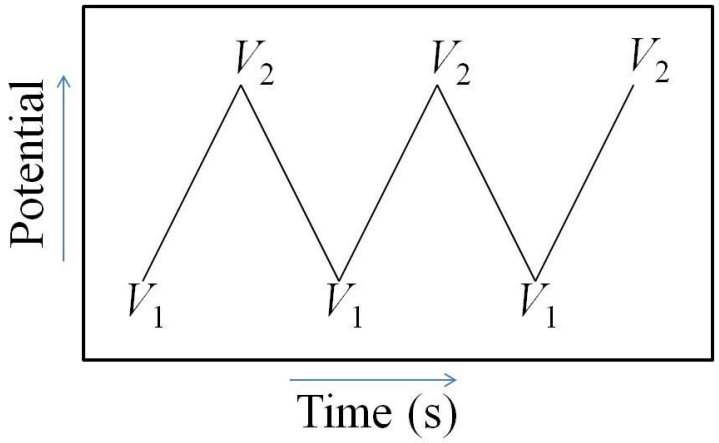

Figure 2.4 Potential waveform during operation time.

Normally, cyclic voltammogram is plotted between current values and potential values. Fig. 2.5 shows the example of cyclic voltammogram of Pt in 0.5M H_2SO_4 at room temperature (VS Ag/AgCl). In the forward sweep, there are three major zones occur as following below;

- H desorption zone
- Double-layer zone
- Pt oxidation zone

In reverse sweep also have three major zones as following below;

- H adsorption zone
- Double-layer zone
- Pt oxide reduction zone

From Fig. 2.5, the H adsorption/desorption peaks are observed at lower potential range and Pt oxidation/Pt oxide reduction peaks are observed at the higher potential range. When the potential is positively scanned, starting from 0.6 V the Pt surface starts to be oxidized to form Pt oxide on Pt surface. On the other hand, when the potential is negatively back scanned, starting from 0.8 V the Pt oxide starts to reduce to bare Pt surface.

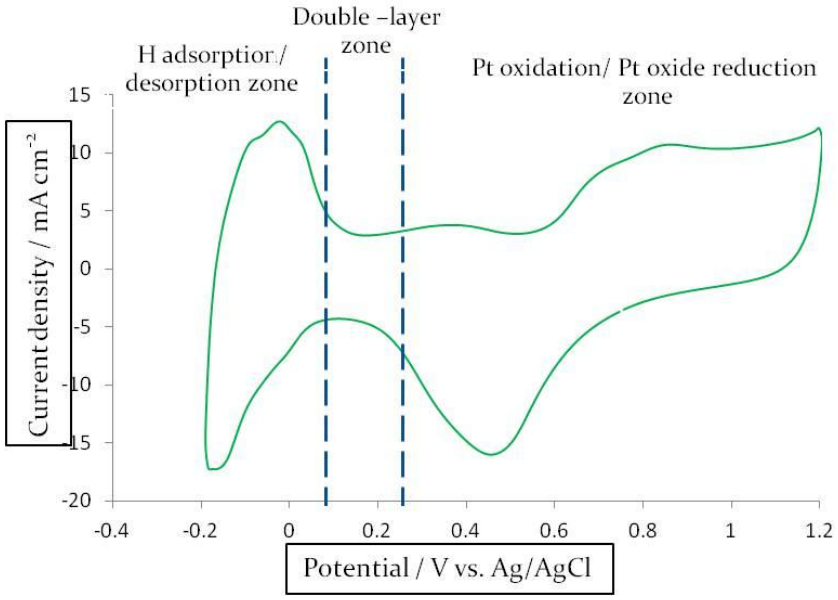

Fig. 2.5 Cyclic voltammogram of Pt/C in N_2-purged 0.5 M H_2SO_4 at room temperature, at a scan rate of 50 mV s^{-1} between -0.2 and 1.20 V (V/ vs Ag/AgCl).

Cyclic voltammetry measurement setup is shown in Fig. 2.6. The unit cell which used for electrochemical measurement consists of three electrodes 1) working electrode, 2) counter electrode (Pt wire) and 3) reference electrode (saturated Ag/AgCl electrode). The electrolyte in measurement can be acidic or basic depend on the application of catalyst. Before start cyclic voltammetry (CV) measurement, we have to clean surface of a glassy carbon disk electrode (3 mm diameter) which was used as the substrate for the catalysts (working electrode) by polishing. The procedure of cyclic voltammetry measurement as following below;

- The catalyst is dispersed in ethanol, and 5% Nafion using an ultrasonic device about 20 minutes to prepare the catalyst ink.
- The ink was dropped on the glassy carbon electrode and dried in atmosphere air until the ink is completely dried.
- The electrolyte was purged under N_2 until 30 minutes.
- The working electrode was put in acidic solution (0.5 M H_2SO_4) which purged with N_2. The scan rate of potential is fixed at 50 mV s^{-1}. The operation temperature is room temperature. The range of potential is fixed between -0.2 and 1.20 V.
- Three electrodes are connected to potentiostat device.
- The samples are measured by CV.

Prior to the CV measurement, the catalyst on glassy carbon electrode was cleaned to remove contaminates on catalyst surface by scanning potential between -0.2V to 1.2V for 30 cycles.

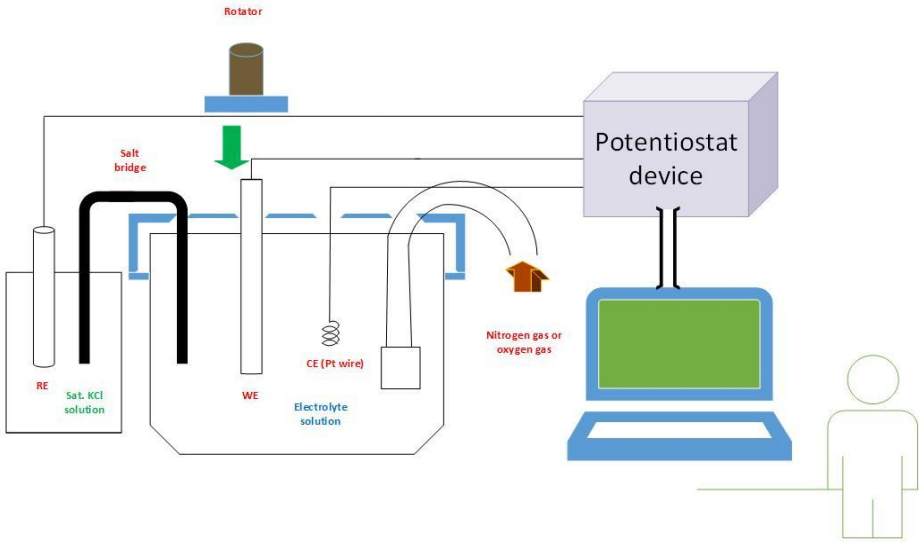

Fig. 2.6 Cyclic voltammetry measurement setup.

2.4.2 Rotating disk electrode (RDE) measurement

For Rotating disk electrode (RDE) measurement setup is similar to cyclic voltammetry setup. Just the working electrode is connected with rotator. The unit cell which used for electrochemical measurement consists of three electrodes 1) working electrode (glassy carbon disk electrode (5 mm diameter)), 2) counter electrode (Pt wire) and 3) reference electrode (saturated Ag/AgCl electrode). The electrolyte in measurement can be acidic or basic depend on the application of catalyst. Before start Rotating disk electrode (RDE) measurement, we have to clean surface of a glassy carbon disk electrode (5 mm diameter) which was used as the substrate for the catalysts (working electrode) by polishing. This measurement can determine the polarization curves for the ORR. The procedure of RDE measurement as following below;

- The catalyst is dispersed in ethanol, and 5% Nafion using an ultrasonic device about 20 minutes to prepare the catalyst ink.
- The ink was dropped on the glassy carbon electrode and dried in atmosphere air until the ink is completely dried.
- The electrolyte was purged under O_2 until 30 minutes.
- The working electrode was put in acidic solution (0.5 M H_2SO_4) which purged with O_2. The scan rate of potential and rotation rate of electrode are fixed at 10 mV s^{-1} and 1600 rpm, respectively. The operation temperature is room temperature. The range of potential is fixed between 0.22 V and 1.0V.
- Three electrodes are connected to potentiostat device.
- The samples are measured by LSV.

2.4.3 Durability test of catalytic performance

The durability of catalyst can evaluate from cyclic voltammogram (Fig. 2.7). All experiments, the working electrode were put in acidic solution (0.5 M H_2SO_4) which purged with N_2. The scan rate of potential is fixed at 50 mV s^{-1}. The operation temperature is room temperature. The range of potential is fixed between -0.2 and 1.20 V.

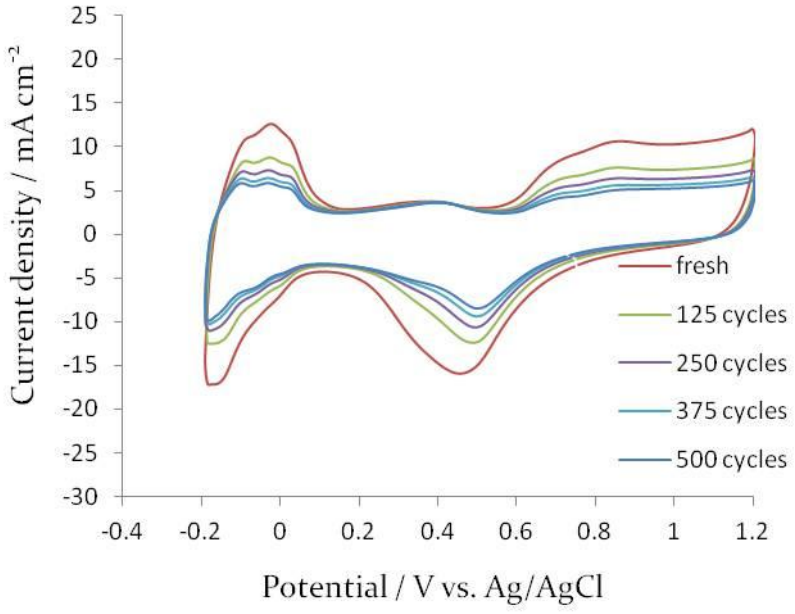

Fig. 2.7 Potential cycling in the durability test

Fig. 2.8 shows hydrogen desorption region which use to determine electrochemically active surface area (ECSA). Due to the exactly amount layer of hydrogen which adsorbed on Pt surface is unknown. So, the calculation of ECSA values based on one layer of hydrogen which adsorbed on Pt surface.

The ECSA was calculated using

$$ECSA = \frac{Q_H}{2.1 \times m_{Pt}} \ , \qquad (1)$$

where Q_H is the integral of the hydrogen desorption peak on the Pt surface (C m^{-2}), 2.1 is the charge required to oxidize a monolayer of hydrogen on the Pt surface (C m^{-2}), and m_{Pt} is the amount of Pt loaded on the glassy carbon electrode (g m^{-2}) [6,7].

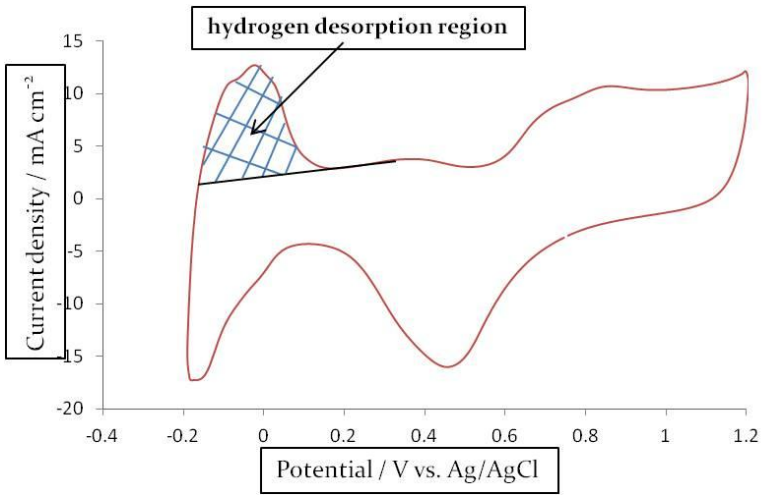

Fig. 2.8 Cyclic voltammogram of Pt/C in N_2-purged, 0.5 M H_2SO_4 at room temperature

References

[1] C. Terashima, Y. Iwai, S. P. Cho, T. Ueno, N. Zettsu, N. Saito, O. Takai, Int. J. Electrochem. Sci. **8**, 5407 (2013).

[2] J. Kang, O. L. Li, N. Saito, Nanoscale **5**, 6874 (2013).

[3] O. Takai, Pure Appl. Chem. **80**, 2003 (2008).

[4] H. O. L. Li, J. Kang, K. Urashima, N. Saito, J. Inst. Electrostat. Jpn. **37**, 22 (2013).

[5] D. A. Skoog, F. J. Holler, T. A. Nieman, "Principles of Instrumental Analysis**",** Saunders College Publishing, 1998.

[6] Y. Liu, J. Chen, W. Zhang, Z. Ma, G.F. Swiegers, C.O. Too, G.G. Wallace, Chem. Mater. **20**, 2603 (2008).

[7] B. Lim, X. Lu, M. Jiang, P.H.C. Camargo, E.C. Cho, E.P. Lee, Y. Xia, Nano Lett. **8**, 4043 (2008).

Chapter 3

~ Highly durable silica coated Pt/Cs with different surfactant types for proton exchange membrane fuel cell application ~

~ Highly durable silica coated Pt/Cs with different surfactant types for proton exchange membrane fuel cell application~

3.1 Introduction

Proton exchange membrane fuel cells (PEMFCs) has many advantages because low temperature operation is available, low emissions are generated from this device and this reaction convert to electrical energy with high efficiency [1,2]. In the present, it is well known that the Pt supported on carbon materials are used be commercially catalyst in PEMFC. The dissolution of Pt nanoparticles contributes to deactivation of catalyst in acidic electrolytes [3-6]. The degradation phenomena of catalyst in fuel cell can occur such as Platinum dissolved in acidic electrolyte, Pt nanoparticles moved to together each others to form big particles, Pt nanoparticles removed from carbon support and Ostwald ripening. To solve the problem, the metal elements such as gold, cobalt and palladium which formed with Pt to be alloy catalysts have been studied [7-10].

Toda *et al.* investigated Pt alloys which were formed between nickel, cobalt, iron and platinum to determine electrocatalytic activity compared with pure Pt-catalysts. In case of Ni-Pt alloy was found that at content of Ni is approximately 30%, the activity exhibited maximum activity. Moreover, Co-Pt alloy which approximately 40% content of Co showed the maximum activity and the last Fe-Pt alloy was observed at approximately 50% content of Fe had maximum activity. B. Lim *et al.* found that the alloy between Pd and Pt which formed nanodendrites shape had higher activity than Pt/Cs about two and a half times base on the same amount of Pt. If the activity compared with Pt-black catalyst, the alloy between Pd and Pt which formed nanodendrites shape shows five times. The alloy catalysts have higher activity and durability compared to that of pure Pt catalysts. However, the metal elements which formed with Pt to be alloy catalysts still dissolve in acidic electrolyte at the cathode electrode. The dissolution of the non-noble transition metal also contributes to deactivation of the catalysts. The polymer electrolyte membrane could be deposited from the dissolved metal elements, which membranes will loss ability to transfer proton [11-13]. In this study, silica was synthesized to cover Pt-based catalysts (1) to avoid the agglomeration of the Pt nanoparticles and (2) to prevent Pt nanoparticles removed from carbon supports. This study is expected to provide an alternative solution for high durability electrode material for PEMFC.

3.2 Experimental details

3.2.1 Catalyst preparation

In this study, silica coated Pt/Cs was synthesized by sol-gel method with three different types of surfactant. Commercial Pt/C catalysts were dispersed in 100 mL surfactant solutions (Cetyltrimethylammonium bromide (CTAB), Sodium dodecylbezenesulfonate (SDBS), and Pluronic 123 (P123)) by sonication for 1 hour. Then 0.1 M NaOH solutions were added to adjust pH to pH 10 and stirred for 5 minutes. Finally, 100 μL triethyl orthosilicate (TEOS) in 2 mL ethanol (EtOH) was injected and stirred for 2 hours. The sample was filtrated and washed several times by distilled water prior to drying at 80 ºC for 6 hours.

3.2.2 Characterization of catalysts

Before measurement, the samples should be fine powder by grinding. The fine powder is spread on film with smoothly surface. The content of SiO_2 in silica coated Pt/Cs with three different types of surfactant was evaluated by X-ray fluorescence spectroscopy (XRF).

The morphology and particle size of Pt nanoparticles were examined by transmission electron microscopy (TEM) which were measured in case of before and after silica coating in durability test. The voltage in measurement was accelerated to 200 kV. The TEM images of the samples were recorded with a JEM-2500SE.

Electrochemical measurements, the unit cell which used for electrochemical measurement consists of three electrodes 1) working electrode, 2) counter electrode (Pt wire) and 3) reference electrode (saturated Ag/AgCl electrode). The electrolyte in measurement can be acidic or basic depend on the application of catalyst. Before start cyclic voltammetry (CV) measurement, we have to clean surface of a glassy carbon disk electrode (3 mm diameter) which was used as the substrate for the catalysts (working electrode) by polishing. First the catalyst is dispersed in ethanol, and 5% Nafion using an ultrasonic device about 20 minutes to prepare the catalyst ink. The ink was dropped on the glassy carbon electrode and dried in atmosphere air until the ink is completely dried. The electrolyte was purged under N_2 until 30 minutes. The working electrode was put in acidic solution (0.5 M H_2SO_4) which purged with N_2. The scan rate of potential is fixed at 50 mV s^{-1}. The operation

temperature is room temperature. The range of potential is fixed between -0.2 and 1.20 V. Three electrodes are connected to potentiostat device. The samples are measured by CV. Prior to the CV measurement, the catalyst on glassy carbon electrode was cleaned to remove contaminates on catalyst surface by scanning potential between -0.2V to 1.2V for 30 cycles. Cyclic voltammogram were used to evaluate electrochemically active surface area (ECSA) and normalized electrochemically active surface area (N-ECSA) of Pt nanoparticles.

3.3 Results and discussion

3.3.1 Proposed mechanism of silica coating of Pt/Cs with various surfactant

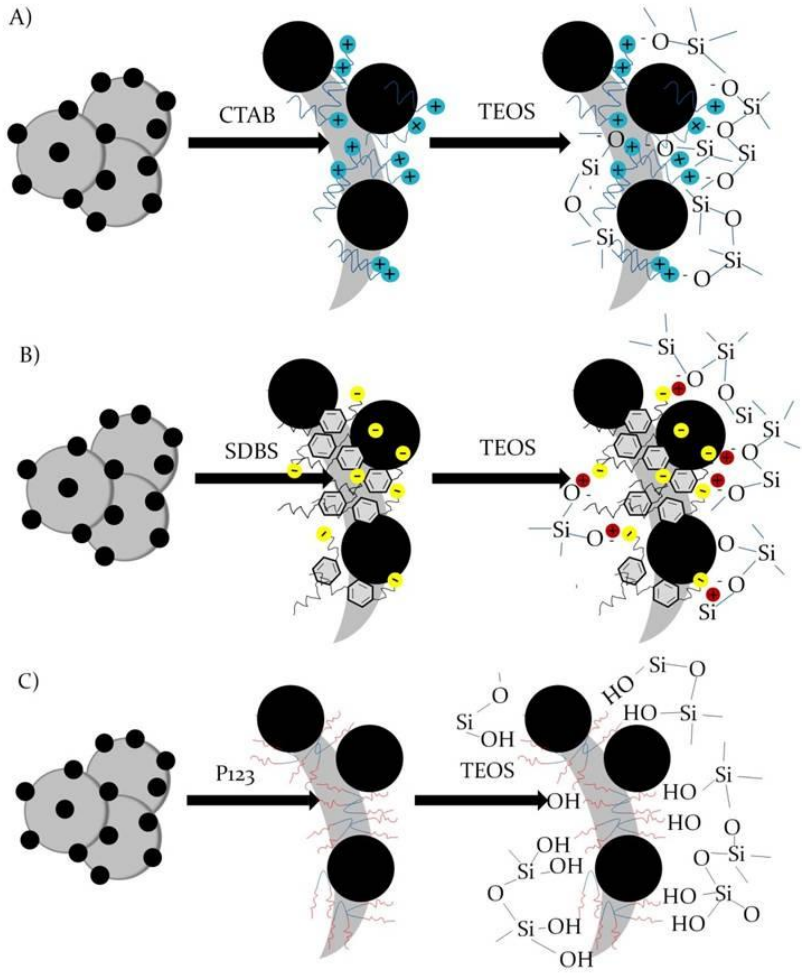

Fig. 3.1 Schematic drawing of possible silica coated Pt/Cs mechanism.

The mechanism of the silica coating on Pt/C is depended on the type of surfactant applied for the coating process. Three kinds of surfactant with different properties were chosen for this study (1) CTAB, a cationic surfactant which consists of positively charged head-group with hydrophilic nature and a hydrophobic tail. (2) SDBS, an anionic surfactant which consists of negatively charged head-group with hydrophilic nature and a hydrophobic tail, and (3) P123, a non-ionic surfactant which consists of polyethylene glycol with hydrophilic nature and polypropylene glycol with hydrophobic nature.

The mechanism of the growing of CTAB is suggested as follows (Fig. 3.1A): the surfactant was adsorbed on Pt/C surface due to the hydrophobic bonding and electrostatic bonding. The surfactant induced nucleation of silica precursor and grew onto the silica by electrostatic interaction between positively charge of surfactant and negatively charge of silica. In the case of SDBS (Fig. 3.1B), the surfactant was adsorbed on Pt/C surface by π-π bonding and hydrophobic bonding. Since the surfactant and silica were both negative charge, a positive charged mediator (Na+) was required to establish the electrostatic interaction between silica and SDBS. If the surfactant was changed to P123 (Fig. 3.1C), it behaved a different mechanism compared to that of CTAB and SDBS. P123 was firstly adsorbed on Pt/C surface by hydrophobic bonding, followed by the nucleation of silica precursor. The silica and surfactant was then bonded by hydrogen bonding. The formation of hydrogen bonding can be direct by bulk water between ether group of P123 and silanol (Si-OH) group of silica.

3.3.2 Morphology of silica-coated Pt particles

Fig. 3.2 shows TEM images of Pt/Cs and silica coated Pt/Cs prepared at different surfactant. The Pt particles size of Pt/Cs before silica coating was about 3.8∓1.3 nm and the Pt particles size after silica coating with CTAB, SDBS, and P123 were 4.0∓1.5 nm, 3.9∓1.5 nm, and 3.8∓1.7 nm, respectively. It means that silica coating was not effect to Pt particles size of Pt/Cs. Silica also was confirm by using Energy-dispersive X-ray spectroscopy (EDS) as shown in supplementary data.

Table 1 presents the SiO_2 contents in various silica coated Pt/Cs samples prepared with different types of surfactant. The amount of silica was contained in Pt/Cs depend on the charge of surfactant. The cationic surfactant could introduce silica on Pt/Cs higher than the anionic surfactant and non-ionic surfactant, respectively.

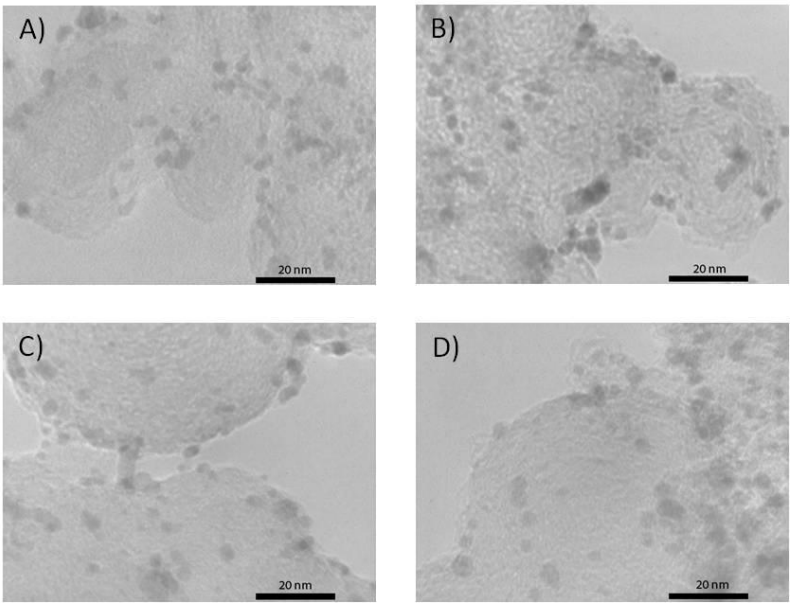

Fig.3.2 TEM images of Pt/Cs before and after silica coating with different surfactant A)Pt/Cs before silica coating, B) silica coated Pt/Cs with CTAB, C) silica coated Pt/Cs with SDBS, C) silica coated Pt/Cs with P123.

Table 1
Contents of SiO_2 in silica coated Pt/Cs with different types of surfactant.

Sample	*Content of SiO_2 (wt %)*
Silica coated Pt/Cs-CTAB	7.40
Silica coated Pt/Cs-SDBS	5.80
Silica coated Pt/Cs-P123	2.32

3.3.3 Electrochemical analyses

Normally, potential cycling is used to measure the durability of Pt/Cs in acid media solution [21-23]. Fig. 3.3 shows CVs of Pt/Cs and silica coated Pt/C with different surfactant during the durability tests. The range of potential of these catalysts was swept between -0.2 and 1.20 V which N_2 purged in acidic electrolyte (0.5 M H_2SO_4). The peak of adsorbed and desorbed hydrogen on Pt surface were found in cyclic voltammogram at -0.2 to 0.1 V and the oxidation and reduction of Pt metal peak also were found in cyclic voltammogram [24, 25]. After finish the durability test (500 cycles), the peak current density of Pt/Cs was significantly decreased. These results indicate that Pt metal particles in Pt/Cs were highly agglomerated and detached from carbon supports in H_2SO_4

electrolyte. On the other hand, the peak of adsorbed and desorbed hydrogen on Pt surface were also observed in the CVs for all silica coated Pt/Cs with different surfactant including the oxidation and reduction of Pt metal peak. The peak currents in the CVs for silica coated with CTAB were similar to that of Pt/Cs but in the case of SBDS and P123, they were significantly higher than Pt/Cs. Therefore, the coverage with silica by using SDBS and P123 improves the durability of Pt/Cs. This result is in agreement with the finding of Takenaka et al. [24-26] in which durability of silica coated Pt/Cs was increased from that of non-coated Pt/Cs. In their case, hydrolysis of 3-aminopropyltriethoxysilane and tetraorthosilicate was used for the silica coating without any usage of surfactants. Takenaka *et al*. have examined the catalytic activity of silica coated Pt catalyst; the silica coated Pt catalysts and non-coated Pt catalyst catalytic activity is no different [24, 27].

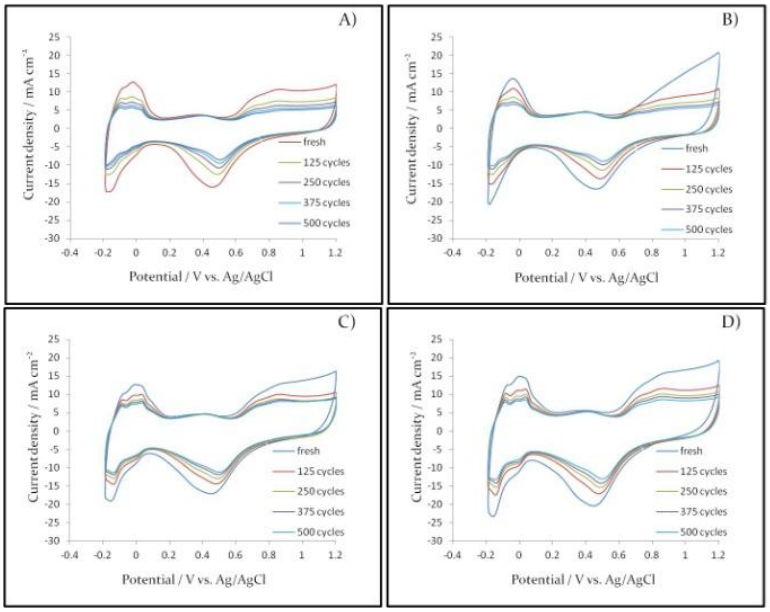

Fig.3.3 CVs for Pt/Cs and silica coated Pt/Cs with different surfactant in N_2-purged 0.5 M H_2SO_4 during the durability tests A) Pt/Cs, B) silica coated with CTAB, C) silica coated with SDBS, D) silica coated with P123

The TEM images of Pt/Cs and silica coated Pt/Cs with different surfactant after the durability tests shown in Fig. 3.4. For Pt/Cs without silica coating (Fig. 3.4A)), we observed severe nanoparticle detachment from carbon supports after 500 cycles. In contrast, silica coated Pt/Cs with different surfactant significantly has successfully secured the Pt nanoparticles on carbon supports. The mechanism which was proposed in Fig. 3.1 seems realistic. However, the images demonstrated certain degree of agglomeration of Pt nanoparticles. The agglomeration of Pt particles of silica coated Pt/Cs

with CTAB was obviously higher than that of silica coated Pt/Cs with SDBS and silica coated Pt/Cs with P123. Therefore, silica coating indicates clearly prevent the Pt particles detachment from carbon supports. In Section 3.3.1, we have discussed the mechanism of silica coating of Pt/Cs with various types of surfactant. The silica coating was either bonded to the Pt/C surface by electrostatic interaction for charged surfactant (CTAB and SDBS) or hydrogen bonding (P123). This bonding is relatively strong and it might secure the position of small Pt NPs on carbon during extreme condition such as acidic environment. As a result, agglomeration or detachment can be successfully avoided.

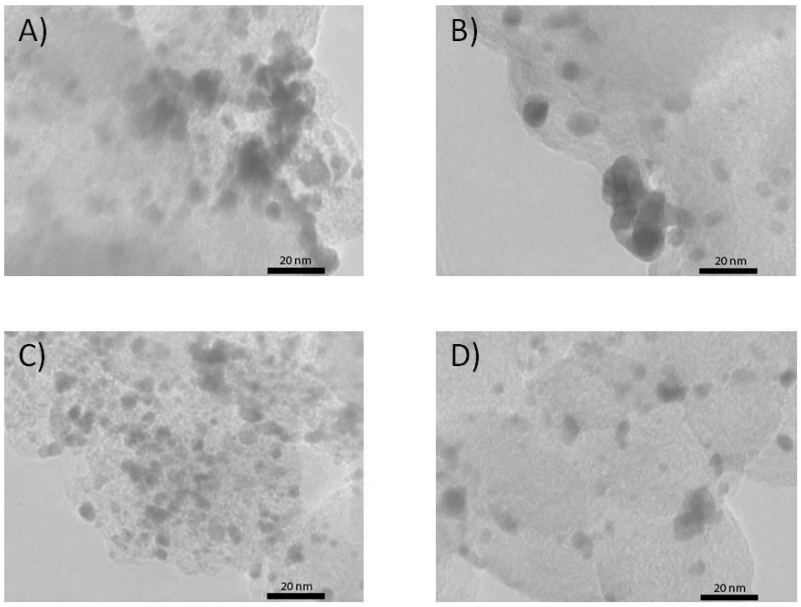

Fig. 3.4 TEM images of A) Pt/Cs, B) silica coated Pt/Cs with CTAB, C) silica coated Pt/Cs with SDBS, D) silica coated Pt/Cs with P123 after the durability tests 500 cycles.

Figure 3.5 shows the change of ECSA of each Pt catalyst after 500 cycle's tests. The ECSA of Pt/Cs was about 66 m^2 $g\text{-}Pt^{-1}$ before testing. The fresh silica coated Pt/Cs-CTAB, silica coated Pt/Cs-SDBS and silica coated Pt/Cs-P123 catalyst had a smaller ECSA (57, 62 and 63 m^2 $g\text{-}Pt^{-1}$, respectively) than the fresh Pt/CS catalyst. After 125 cycles, All silica coated Pt/Cs had a larger ECSA than Pt/Cs. After 500 cycles, silica coated Pt/Cs-SDBS and silica coated Pt/Cs-P123 catalyst still had a larger ECSA than Pt/Cs. The Normalized electrochemically active surface area (N-ECSA) of Pt metal particles for each Pt catalyst was evaluated from each cyclic voltammogram as shown in Fig. 3.3. The results are summarized in Fig. 3.6.

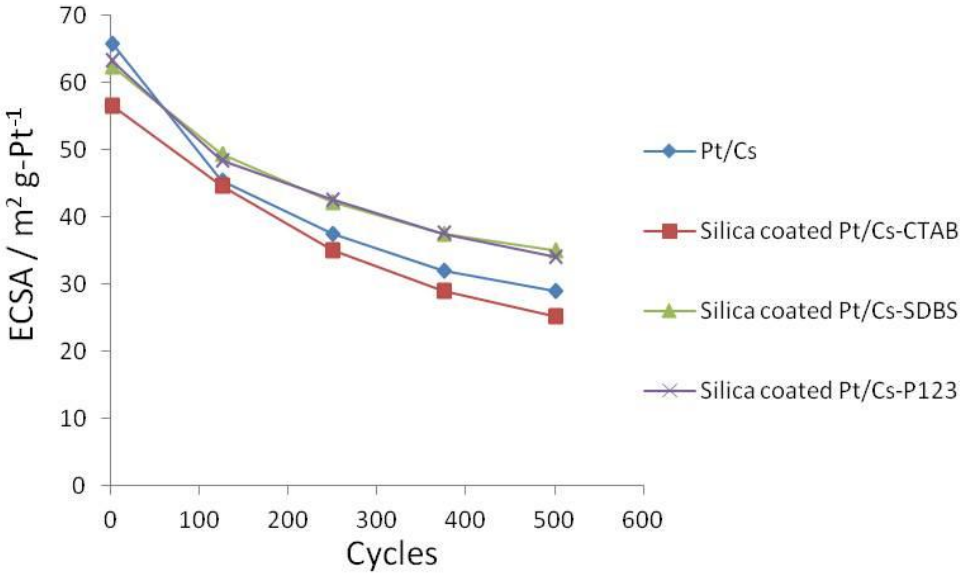

Fig. 3.5 The electrochemically active surface area for Pt/Cs and silica coated Pt/Cs with different surfactant during the durability tests

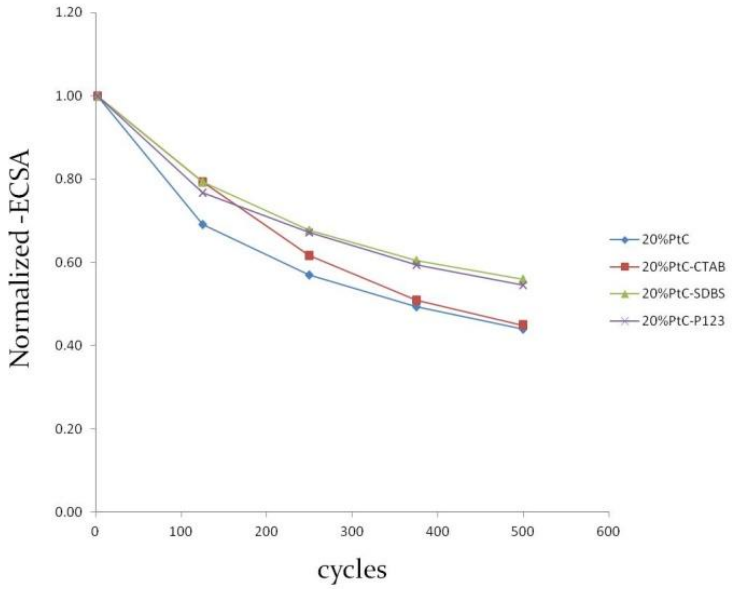

Fig. 3.6 Normalized electrochemically active surface area for Pt/Cs and silica coated Pt/Cs with different surfactant during the durability tests.

Fig. 3.6 shows that from the initial to 500 potential cycling, N-ECSA of Pt/Cs exhibited lowest surface area compared to silica coated Pt/Cs. The N-ECSA for Pt/Cs was reduced to 0.44 after 500 cycles. The N-ECSA for fresh silica coated Pt/Cs with CTAB, SDBS, and P123 were reduced to 0.45, 0.56, and 0.54 after 500 cycles, respectively. Fig. 3.7 shows the Zeta potential of Pt/Cs in different pH, when pH changes from basic to acid condition, the Zeta potential has a tendency from negative to positive. As a result, there is the repulsion force between positively charge of surfactant, positively charge of Pt/Cs (pH<1), and positively charge of silica in acid condition (pH <2) [28] during the durability test which affect to no significantly durable enhancement in case of CTAB. However, the silica coated Pt/Cs with SDBS and P123 thus maintains the active surface area of Pt which is higher than Pt/Cs about 27.3% and 22.7%, respectively.

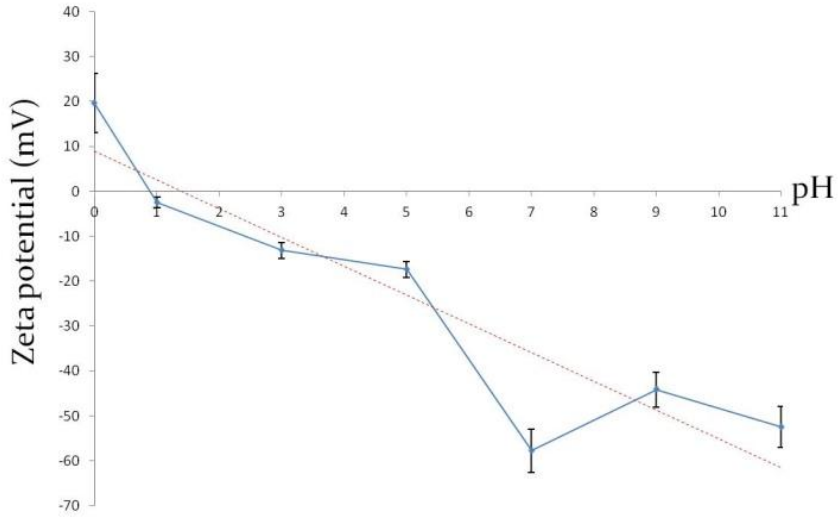

Fig.3.7 Zeta potential of Pt/Cs dispersed in water with different pH.

3.4 Conclusion

Silica coated Pt/Cs catalysts by sol-gel method for PEMFCs application has shown improvement of the catalysts durability under acidic condition. The degree of improvement depended on the type of surfactant applied in the coating method. Silica coated Pt/Cs by SDBS and P123 improved the durability by 27.3% and 22.7%, respectively, compared to that of non-coated Pt/Cs after 500 cycles in CV test under 0.5M H_2SO_4 electrolytes. The N-ECSA of silica coated Pt/Cs by using SDBS and P123 was higher than that of non-coated Pt/Cs by preventing agglomeration and detachment of Pt nanoparticles from carbon support.

References

[1] M. K. Debe, *Nature,* 2012, 486, 43-51.

[2] "The Fuel Cell Industry Review 1012", *Fuel Cell Today*, Royston, Hertfordshire, UK, 2012

[3] J. Willsau, J. Heitbaum, *J. Electroanal. Chem*., 1984, 161, 93-101.

[4] A. Honji, T. Mori, K. Tamura, Y. Hishimura, *J. Electrochem. Soc*., 1988, 135, 355-359.

[5] A. C. C. Tseung, S. C. Dhara, *Electrochimica Acta*, 1975, 20, 681-683.

[6] G. A. Gruver, R. F. Pascoe, H. R. Kunz, *J. Electrochem. Soc*., 1980, 127, 1219-1224.

[7] T. Toda, H. Igarashi, H. Uchida, M. Watanabe, *J. Electrochem. Soc*., 1999, 146, 3750-3756.

[8] V. R. Stamenkovic, B. S. Mum, M. Arenz, K. J. J. Mayrhofer, C. A. Lucas, G. Wang, P. N. Ross, N. M. Markovic, *Nat. Mater.*, 2007, 6, 241-247.

[9] S. Takenaka, A. Hirata, E. Tanabe, H. Matsune, M. Kishida, *J. Catal*., 2010, 274, 228-238.

[10] B. Lim, M. Jiang, P. H. Camargo, E. C. Cho, J. Tao, X. Lu, Y. Zhu, Y. Xia, *Science*, 2009, 324, 1302-1305.

[11] T. Kunimoto, M. Inaba, Y. Nakayama, K. Ogata, R. Umebayashi, A. Tasaka, Y. Iriyama, T. Abe, Z. Ogumi, *J. Power Sources*, 2006, 158, 1222−1228.

[12] E. Guilminot, A. Corcella, F. Charlot, F. Maillard, M. Chatenet, *J. Electrochem. Soc*., 2007, 154, B96−B105.

[13] T. Okada, Y. Ayata, H. Satou, M. Yuasa, I. Sekine, *J. Phys. Chem. B*, 2001, 105, 6980−6986.

[14] S. H. Wu and P. Pendleton, *J. Colloid Interface Sci*., 2001, 243**,** 306–315.

[15] J. X. Xiao, Y. Zhang, C. Wang, J. Zhang, C. M. Wang, Y. X. Bao, Z. G. Zhao, *Carbon*, 2005, 43, 1032-1038.

[16] S. Zor, *J. Serb. Chem. Soc*., 2004, 69(1), 25–32.

[17] K. Yang, Q. Jing, W. Wu, L. Zhu, B. Xing, *Environ. Sci. Technol.*, 2010**,** *44*, 681–687.

[18] M. S. Sánchez, A. M. Valiente, A. G. Ruiz, D.M. Nevskaia, *J. Colloid Interface Sci*., 2010, 343**,** 194-199.

[19] Q. Huo, D. I. Margolese, U. Ciesla, P. Feng, T. E Gier, P. Sieger, R. Leon, P. M. Petroff, F. Schuth, G. D. stucky, *Nature,* 1994, 368, 317-320.

[20] Q. Huo, D. I. Margolese, U. Ciesla, D. G. Demuth, P. Feng, T. E Gier, P. Sieger, S. A. Firouzi, B. F. Chmelka, Ferdi Schuth, F. Schuth, G. D. stucky, *Chem. Mater.*, 1994, 6, 1176-1191.

[21] A. Kongkanand, S. Kuwabata, G. Girishkumar, P. Kamat, *Langmuir*, 2006, 22, 2392-2396.

[22] Z. Chen, M. Waje, W. Li, Y. Yan, *Angew. Chem. Int. Ed.*, 2007, 46, 4060 –4063.

[23] P. J. Ferreira, G. J. la O, Y. Shao-Horn, D. Morgan, R. Makharia, S. Kocha, H. A. Gasteigerc, *J. Electrochem. Soc*., 2005, 152 (11), A2256-2271.

[24] S. Takenaka, H. Miyamoto, Y. Utsunomiya, H. Matsune, M. Kishida, *J. Phys. Chem.* C, 2014, 118, 774-783.

[25] S. Takenaka, H. Matsumori, H. Matsune, E. Tanabe, M. Kishida, *J. Electrochem. Soc*., 2008, 155 (9), B929-B936.

[26] S. Takenaka, H. Matsumori, K. Nakagawa, H. Matsune, E. Tanabe, M. Kishida, , *J. Phys. Chem.* C, 2007, 111, 15133-15136.

[27] S. Takenaka, T. Miyazaki, H. Matsune, M. Kishida, *Catal. Sci. Technol*., 2015, 5, 1133-1142.

[28] J. A. A. Júnior, J. B. Baldo, *New Journal of Glass and Ceramics*, 2014, 4, 29-37.

Supplementary data

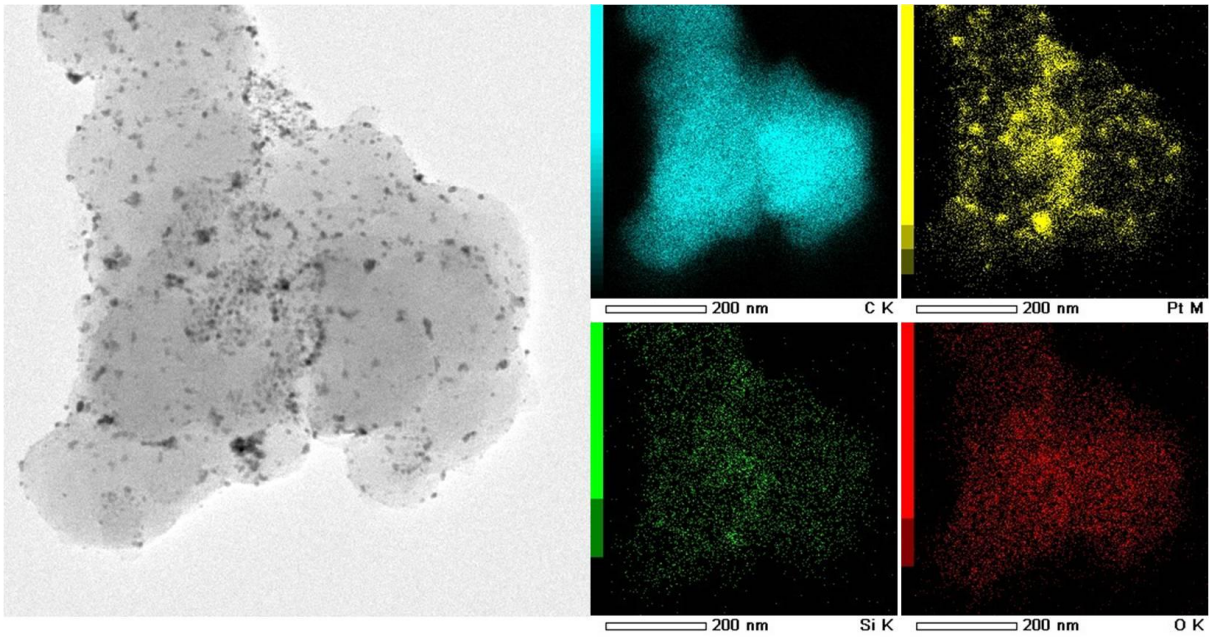

Fig. s-1 STEM image and EDS-mapping of silica coated Pt/Cs by using CTAB.

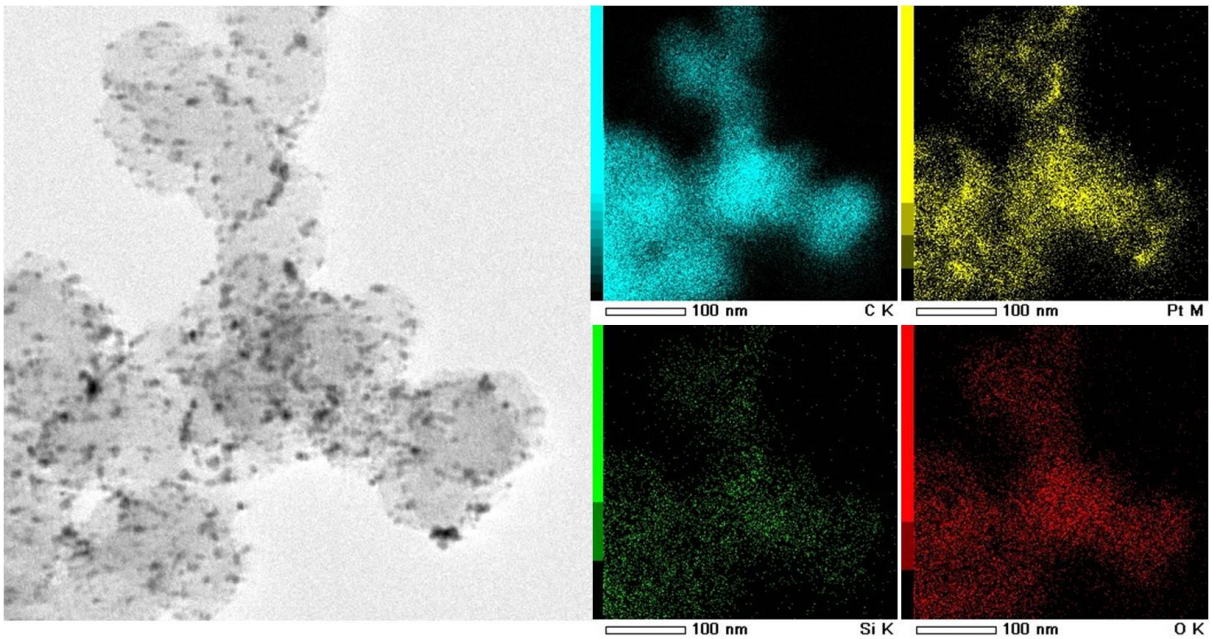

Fig. s-2 STEM image and EDS-mapping of silica coated Pt/Cs by using SDBS.

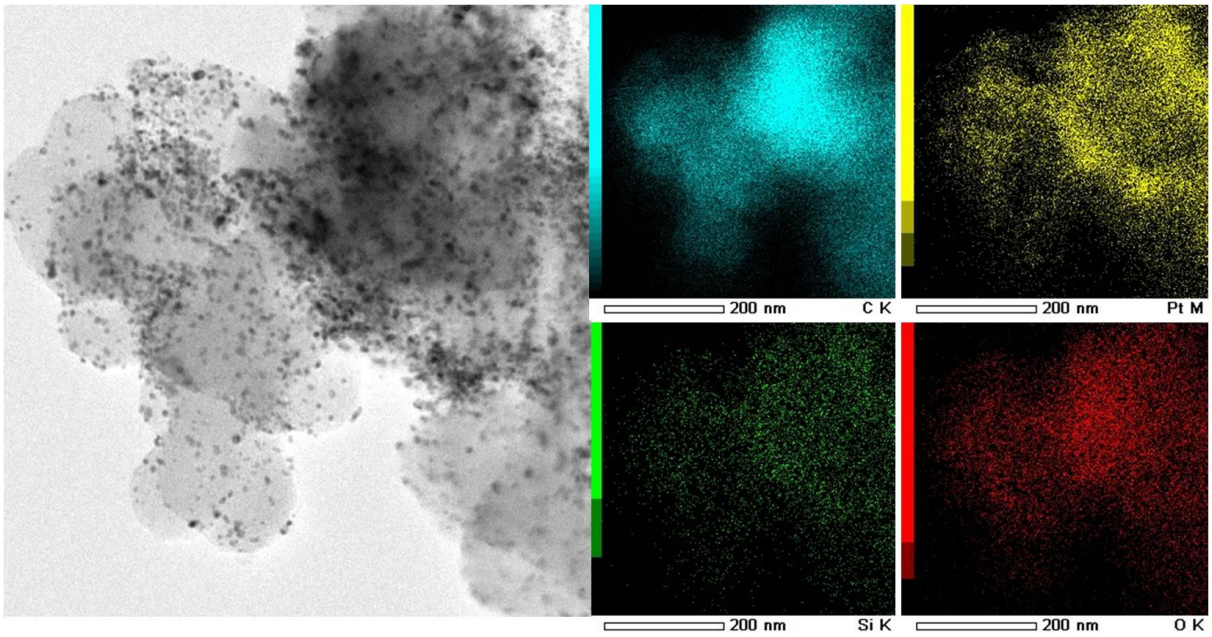

Fig. s-3 STEM image and EDS-mapping of silica coated Pt/Cs by using P 123.

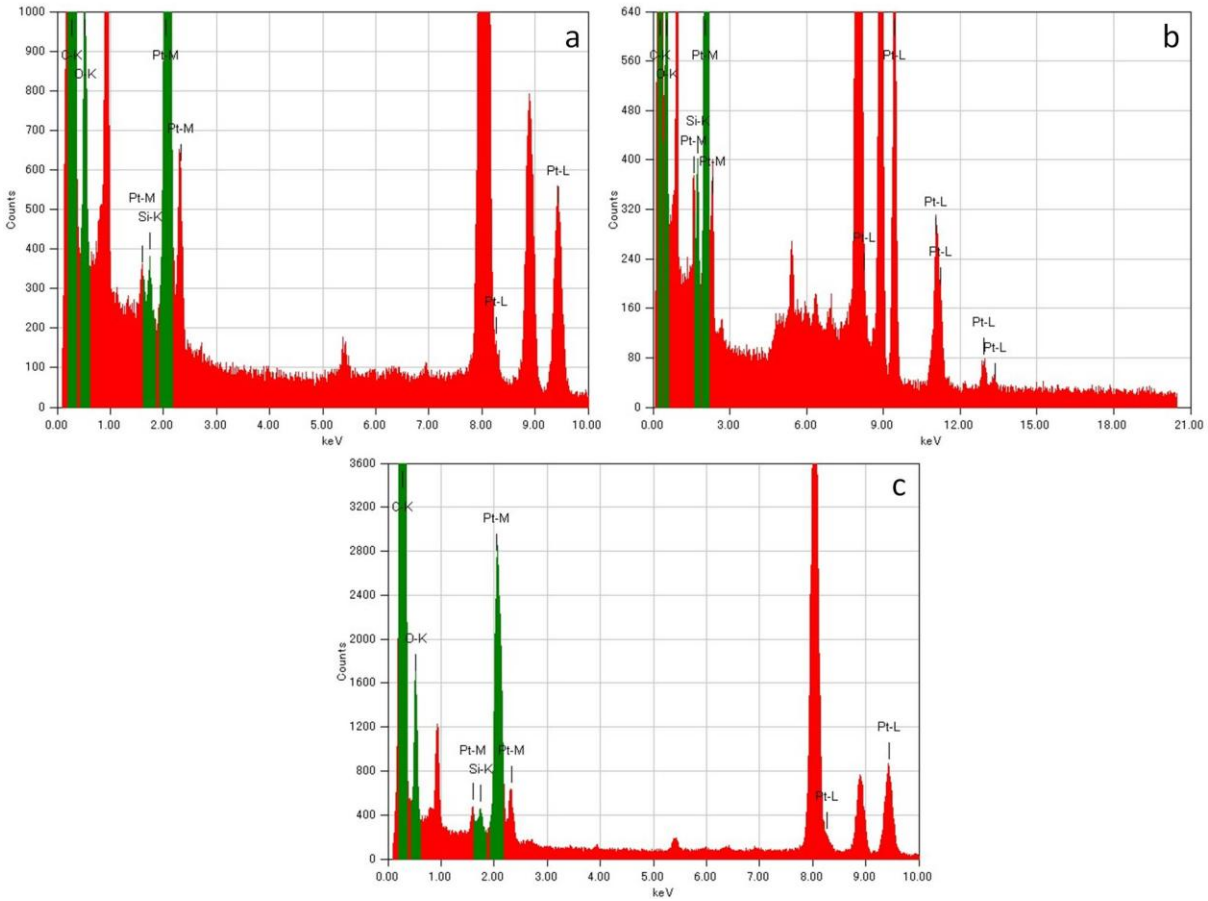

Fig. s-4 Spectra of Si element on silica coated Pt/Cs with different surfactants a) CTAB, b) SDBS and c) P 123.

Chapter 4

~ Highly durable silica-coated Pt/carbon nanotubes for proton exchange membrane fuel cells application ~

~ Highly durable silica-coated Pt/carbon nanotubes for proton exchange membrane fuel cells application ~

4.1 Introduction

Carbon nanotubes (CNTs) are a promising material for many applications owning to their unique electronic and chemical properties [1]. CNTs were widely used in fuel cell, biosensors, catalytic reaction and adsorption applications due to its specific properties [2,3]. Metal nanoparticles supported on CNTs are often used in power generation applications. For example, Pt/CNTs are applied as electrocatalysts in PEMFCs [4-6]. Pt/CNTs show higher activity in oxygen reduction reaction than Pt/carbon black, which have been widely used in PEMFCs [7-9]. However, The Pt nanoparticles could be highly degraded in acidic electrolyte conditions [10-13]. The Pt nanoparticles might dissolved in acidic electrolyte or detach from carbon supports at cathode electrode. Pt nanoparticles can also grow to undesired large particles which affect to the decreasing of active area to react between catalyst, fuel and oxidant by both agglomeration of Pt nanoparticles and Ostwald ripening phenomena. The polymer electrolyte membrane could be deposited from the dissolved metal elements, which membranes will loss ability to transfer proton [14-16].

Takenaka and co-workers have studied silica coating on Pt/CNTs, and in results showed that the silica coating of Pt/CNTs enhanced the durability of the catalyst during the durability test. However, strong and toxic acids such as nitric acid (HNO_3) and sulfuric acid (H_2SO_4), high temperature and long time for consuming are required in Pt/CNT preparation [17,18]. Our group has studied the synthesis of metal nanoparticles supported on carbon using an innovative plasma-in-liquid method, which is known as the [solution plasma process (SPP)] [19,20]. In this process, there is no need high temperature and vacuum condition in operation; no need long time for operation and no need toxic and strong acid which is the advantages of SPP, as compared with the above method. SPP is used to synthesize Pt/CNT catalyst in this study, Pt/CNT and then coated with silica layers to (1) prevent detachment of Pt nanoparticles from CNTs and (2) to avoid the agglomeration of Pt nanoparticles. This study is expected to provide an innovative use of SPP for synthesizing Pt supported on CNTs and coating with silica to enhance the durability of metal based electrochemical catalysts for PEMFC applications.

4.2 Experimental details

4.2.1 Synthesis of Pt nanoparticles on CNTs

In this study, Pt/CNTs were synthesized by SPP. SPP is applied widely for metal nanoparticle synthesis nowadays. The details of SPP, including its mechanism and physical and chemical aspects have been published by the co authors [19-22]. The experimental set up is shown in Fig. 4.1. The system consisted of a pair of platinum electrodes (diameter of 1#mm) placed in a glass vessel (100 ml) and discharged in CNT suspension (0.01g of CNTs in distilled water) for 5, 10, and 15 min. The samples were labeled 5-Pt/CNTs, 10-Pt/CNTs, and 15-Pt/CNTs, respectively.The electrodes were connected to a bipolar–DC pulse power supply for plasma generation. The electrodes were insulated with ceramic tubes. The primary voltage, pulse frequency, pulse width, and electrode distance were fixed at 100 V, 20 kHz, 0.5 μs, and 0.5 mm, respectively.

4.2.2 Synthesis of silica-coated Pt/CNTs

Silica-coated Pt/CNTs were synthesized by the sol-gel method with a cationic surfactant. Pt/CNTs were dispersed in 100 mL of a surfactant solution [cetyltrimethylammonium bromide (CTAB)] by sonication for 1 h. Then 0.1 M NaOH solutions was added to adjust the pH of the solution to 10 and stirred for 5 min. Finally, a mixture of 100 μL of triethyl orthosilicate (TEOS) and 2 mL of ethanol (EtOH) was injected to CNT suspension and stirred for 2 h. The sample was filtrated and washed several times with distilled water, and then dried 80 ºC for 6 hours.

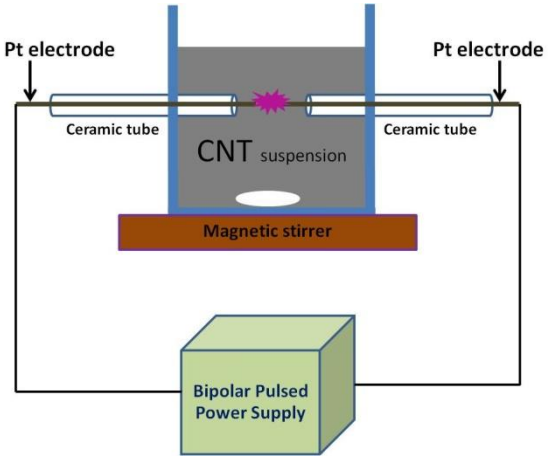

Fig. 4-1 Experiment setup

4.2.3 Characterization of catalysts

The structure of catalyst was characterized by X-ray diffraction (XRD) using an XRD Rigaku Smartlab instrument with Cu Kα radiation (λ = 0.154 nm) in accordance with the standard procedure.

The morphology and particle size of Pt nanoparticles were examined by transmission electron microscopy (TEM) which were measured in case of before and after silica coating in durability test. The voltage in measurement was accelerated to 200 kV. The TEM images of the samples were recorded with a JEM-2500SE.

Electrochemical measurements, the unit cell which used for electrochemical measurement consists of three electrodes 1) working electrode, 2) counter electrode (Pt wire) and 3) reference electrode (saturated Ag/AgCl electrode). The electrolyte in measurement can be acidic or basic depend on the application of catalyst. Before start cyclic voltammetry (CV) measurement, we have to clean surface of a glassy carbon disk electrode (3 mm diameter) which was used as the substrate for the catalysts (working electrode) by polishing. First the catalyst is dispersed in ethanol, and 5% Nafion using an ultrasonic device about 20 minutes to prepare the catalyst ink. The ink was dropped on the glassy carbon electrode and dried in atmosphere air until the ink is completely dried. The electrolyte was purged under N_2 until 30 minutes. The working electrode was put in acidic solution (0.5 M H_2SO_4) which purged with N_2. The scan rate of potential is fixed at 50 mV s^{-1}. The operation temperature is room temperature. The range of potential is fixed between -0.2 and 1.20 V. Three electrodes are connected to potentiostat device. The samples are measured by CV. Prior to the CV measurement, the catalyst on glassy carbon electrode was cleaned to remove contaminates on catalyst surface by scanning potential between -0.2V to 1.2V for 30 cycles. In case of determination of polarization curve, the working electrode was put in acidic solution (0.5 M H_2SO_4) which purged with O_2. The scan rate of potential and rotation rate of electrode are fixed at 10 mV s^{-1} and 1600 rpm, respectively. The operation temperature is room temperature. The range of potential is fixed between 0.22 V and 1.0V. Three electrodes are connected to potentiostat device. The samples are measured by LSV.

4.3 Results and discussion

4.3.1 Characteristics of Pt/CNTs

Pt nanoparticles were synthesized by the sputtering of the electrode under high-voltage discharges during SPP. The structure characterized of Pt nanopaticles was by XRD analysis. The typical XRD patterns are shown in Fig. 4.2. Four peaks were observed at 2θ of ca. 39.7°, 46.2°, 67.4°, and 81.2°, which corresponded to Pt (111), (200), (220), and (311), respectively. These peaks belong to the reflections of the FCC structure of the polycrystalline Pt nanoparticles. The XRD patterns suggest that the Pt nanoparticles were successfully loaded on CNTs by the SPP with 5, 10, and 15 min. The intensity of metal peaks increased with increasing SPP discharge time.

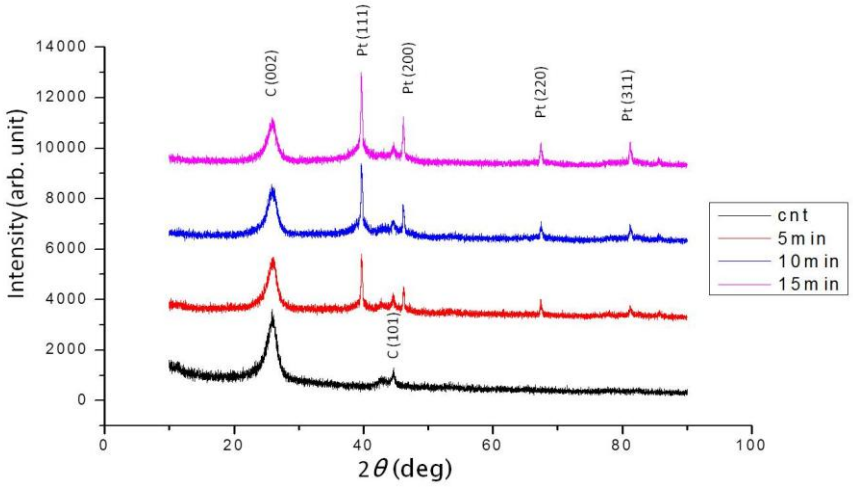

Fig. 4-2 X-ray diffraction patterns of Pt/CNTs

4.3.2 Morphology of silica-coated Pt particles

Figure 4.3 shows the TEM images of Pt/CNTs and silica-coated Pt/CNTs prepared by CTAB. The sized of Pt nanoparticles were similar in size before and after silica coating, as shown in Figs. 4.3(a) and Fig. 4.3(b). This indicates that silica coating has no significant effect on the size of Pt nanoparticles. The sizes of Pt nanoparticles of 15-Pt/CNTs and silica-coated 15-Pt/CNTs were about 4 to 8 nm. A high-magnification TEM image of silica-coated 15-Pt/CNTs is shown in Fig. 4.3(c), which clearly shows that the thickness of the silica layer was in the range from 2 to 4 nm. The amount of Pt

in 15-Pt/CNTs was measured to be 15.67 wt %by inductively coupled plasma atomic emission spectroscopy (ICP-AES) analysis

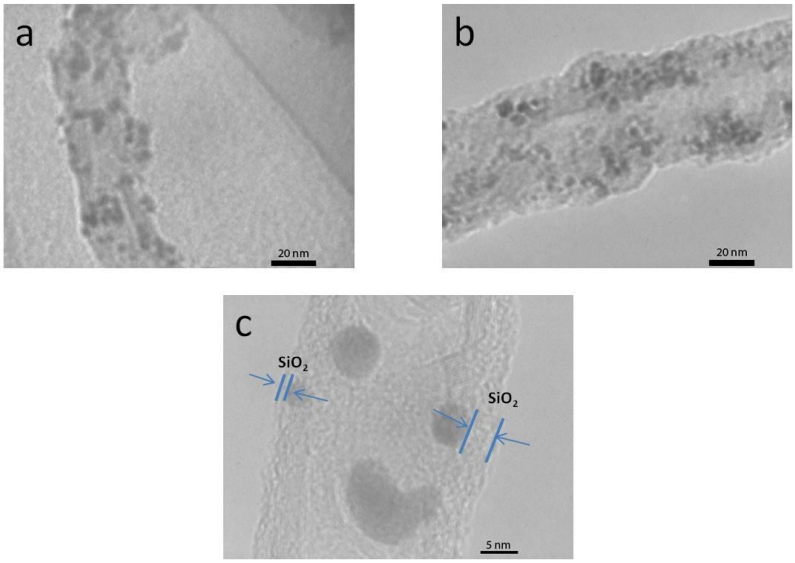

Fig. 4.3 TEM images of 15-Pt/CNTs (a) before and (b, c) after silica coating

4.3.3 Electrochemical analyses

In general, the durability of the catalytic performance of Pt nanoparticle can be examined by potential cycling in an acidic medium solution [22-25]. The commercial 20 wt. % Pt/Vulcan XC-72 (Pt/C) was applied as the reference material for the durability study. All potentials are given relative to reversible hydrogen electrode (RHE). Figure 4.4 shows the corresponding CV results of Pt/C, 15-Pt/CNTs, and silica-coated 15-Pt/CNTs for 100, 200, and 300 cycles. The range of potential of these catalysts was swept between -0.2 and 1.20 V which N_2 purged in acidic electrolyte (0.5 M H_2SO_4). The peak of adsorbed and desorbed hydrogen on Pt surface were found in cyclic voltammogram at -0.02 to 0.3 V and the oxidation and reduction of Pt metal peak also were found in cyclic voltammogram at 0.6 – 1.2 V [18,26]. In Fig. 4.4(a), the peak currents of Pt/C decreased significantly after 300 cycles. In Figs. 4.4(b) and (c), similar peak couples were also observed in the CVs for 15-Pt/CNTs and silica-coated 15-Pt/CNTs. The peak currents of 15-Pt/CNTs also decreased when the cycles increased. However, in the case of silica-coated 15-Pt/CNTs, the decrease in peak current was much less than for other samples. Therefore, the durability of 15-Pt/CNTs was significantly improved silica coating.

Before the durability test, the ORR currents at approximately 0.7 V of 15-Pt/CNTs > Pt/C > silica coated 15-Pt/CNTs but the ORR current of silica coated 15-Pt/CNTs > 15-Pt/CNTs > Pt/C after 300 cycles of the durability test which is shown in Figure 4.5. These results indicate that in long term the catalyst which coated with silica shows better ORR activity than non coating. However, Pt/CNTs still exhibited better than Pt/C.

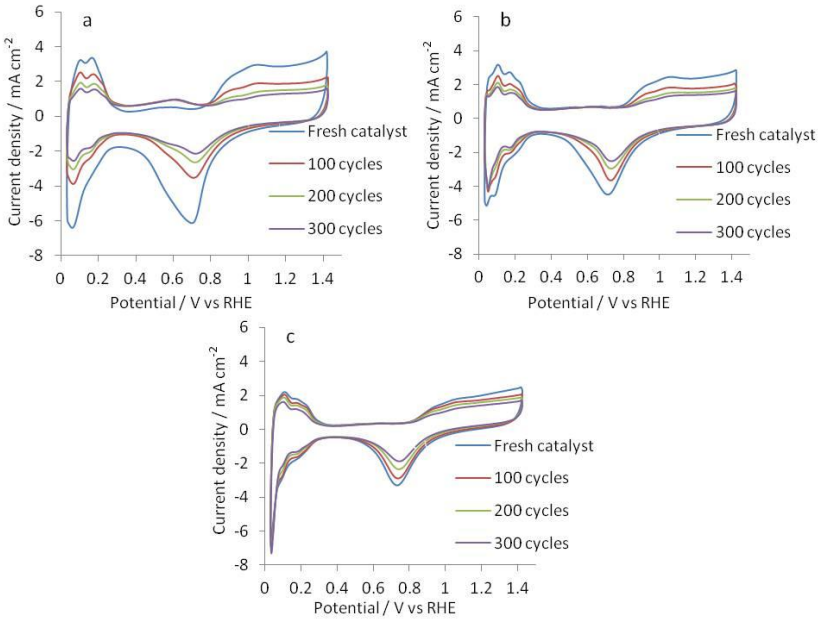

Fig. 4.4 CVs of Pt/C (a), 15-Pt/CNTs (b), and silica-coated 15-Pt/CNTs in N_2-purged 0.5 M H_2SO_4 during the durability tests.

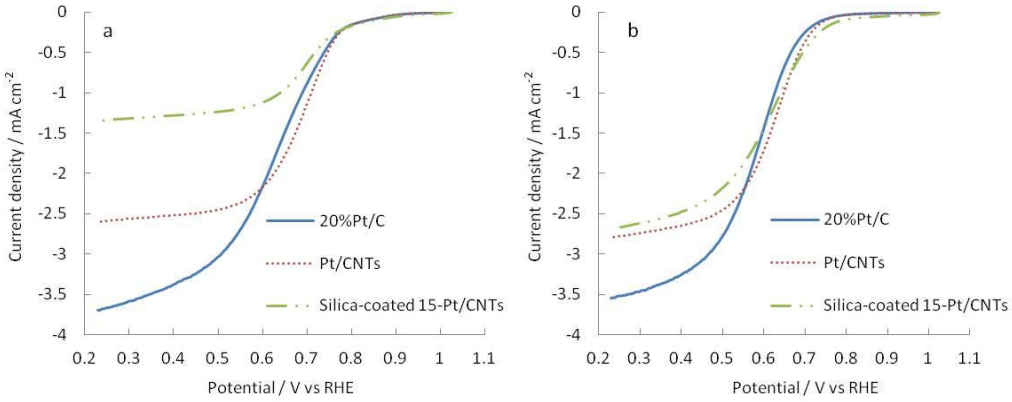

Fig. 4.5 Polarization curves associated with the ORR on Pt/C, 15-Pt/CNTs, and silica-coated 15-Pt/CNTs (a) before and (b) after 300 cycle of durability tests.

Figure 4.5 shows the change of ECSA of each Pt catalyst after 300 cycle's tests. The ECSA of Pt/Cs and Pt/CNTs were about 47 m^2 g-Pt^{-1} and the ECSA of silica-coated 15-Pt/CNTs was about 37 m^2 g-Pt^{-1} before testing. After 100 cycles, 15-Pt/CNTs and silica-coated 15-Pt/CNTs showed larger ECSAs than Pt/C. After 300 cycles, the ECSAs of Pt/C, 15-Pt/CNTs, and silica-coated 15-Pt/CNTs were about 17, 27, and 29 m^2 g-Pt^{-1}, respectively.

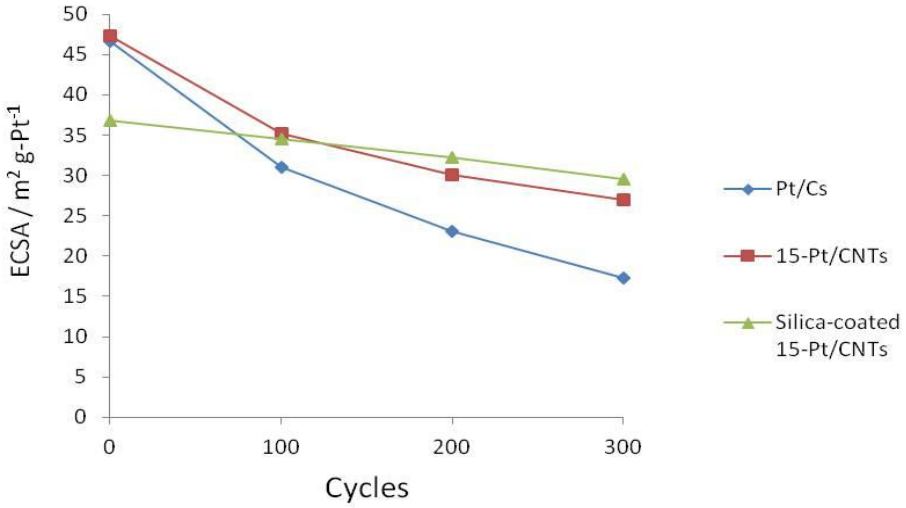

Fig. 4.6 Electrochemically active surface areas of Pt/C, 15-Pt/CNTs, and silica-coated 15-Pt/CNTs during the durability tests

The normalized electrochemically active surface area (N-ECSA) is the ratio of the electrochemically active surface area during *n* number of cycles to the initial electrochemically active surface area, which is calculated using.

$$N - ECSA = ECSA\ (cycle\ n)/ECSA\ (\ initial\ cycle). \qquad (1)$$

Fig. 2.8 shows hydrogen desorption region which use to determine electrochemically active surface area (ECSA). Due to the exactly amount layer of hydrogen which adsorbed on Pt surface is unknown. So, the calculation of ECSA values based on one layer of hydrogen which adsorbed on Pt surface.[27]. The ECSA was calculated using

$$ECSA = \frac{Q_H}{2.1 \times m_{Pt}}\ , \qquad (2)$$

where Q_H is area under peak of desorbed hydrogen from Pt surface (C m^{-2}), 2.1 is the charge required to oxidize a monolayer of hydrogen on the Pt surface (C m^{-2}), and m_{Pt} is the amount of Pt loaded on working electrode (g m^{-2}) [28-30].

Fig. 4.7 shows that from the initial to 300 potential cycling, N-ECSA of Pt/Cs exhibited lowest surface area compared to silica coated Pt/Cs. The results indicate that silica coating can improve the durability of Pt nanoparticles by 43 and 24% compared with Pt/C and 15-Pt/CNTs, respectively.

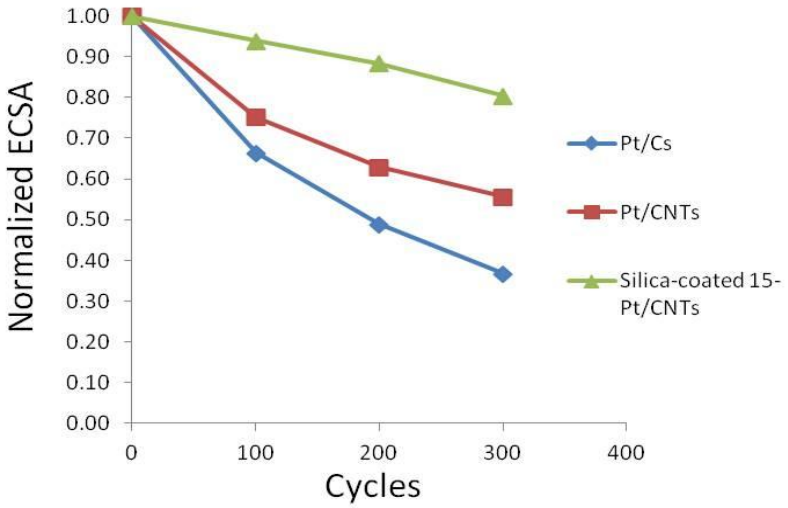

Fig. 4.7 Normalized electrochemical surface areas of Pt/C, 15-Pt/C, and silica-coated Pt/C during the durability tests.

4.3.4 Detachment and agglomeration of Pt nanoparticles after 300 potential cycles

Morphology of silica-coated Pt particles

The TEM images of Pt/C, 15-Pt/CNTs, and silica-coated 15-Pt/CNTs before and after 300 cycles in CVs are shown in Fig. 4.8. For Pt/C, we observed severe nanoparticles detachment from carbon supports, when compared with Figs. 4.8(a) and 4.8(b). After 300 cycles, the large Pt particles of 15-Pt/CNTs were observed since the agglomeration of Pt nanoparticles as shown in Fig. 4.8(d). In contrast, silica coated 15-Pt/CNTs [Fig. 4.8(f)] shows the successful the attachment of the Pt nanoparticles to carbon supports and also no agglomeration of Pt nanoparticles. These results agree with the electrochemical analyses and proved that silica coating was effectively prevents the detachment or agglomeration of Pt nanoparticles.

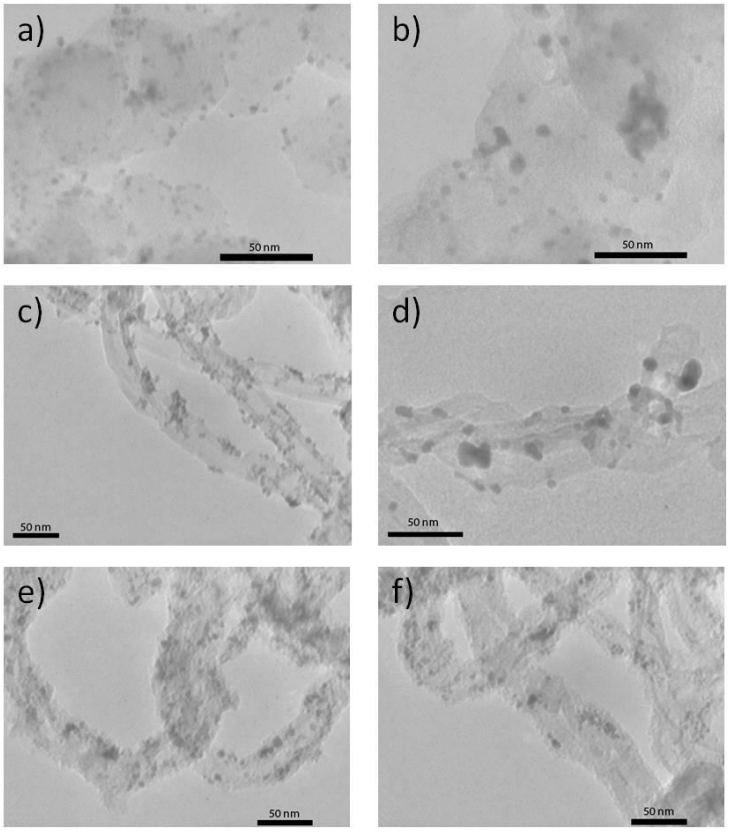

Fig. 4.8 TEM images of (a) Pt/C, (c) 15-Pt/CNTs, (e) silica-coated 15-Pt/CNTs before durability tests and (b) Pt/C, (d) 15-Pt/CNTs, and (f) silica-coated 15-Pt/CNTs after 300 cycles of the durability tests

4.4 Conclusion

We have successfully deposited Pt particles by SPP on CNTs. The synthesized Pt nanoparticles by SPP ranged in size from 4 to 8 nm, and the particle sizes were similar with increasing process time from 5-15 minutes. The amount of Pt in CNTs was 15.67 wt. % after 15 minutes of SPP process. A high-magnification TEM image of silica-coated 15-Pt/CNTs clearly demonstrated that the thickness in the range of 2 to 4 nm of the silica layer was synthesized in this study. Both Pt/CNTs and silica-coated Pt/CNTs showed higher catalytic activity than commercial Pt/C after 300 cycles of durability tests. The durability of 15-Pt/CNTs was higher than that of commercial Pt/C by 19%. Silica-coated 15-Pt/CNTs showed improvement of the catalyst durability under acidic condition by about 43% compared with commercial Pt/C after 300 cycles in the CV test in 0.5#M H_2SO_4 electrolytes. The study has successfully illustrated an innovative and simple method of Pt nanoparticles on CNTs synthesizing, the durability of the material increased by sol-gel coating in an acidic environment. The thin layer of silica coated on Pt/CNTs prevented agglomeration and detachment of Pt nanoparticles from the carbon support.

References

[1] S. Iijima, Nature **354**, 56 (1991).

[2] M. F. L. De Volder, S. H. Tawfick, R. H. Baughman, and A. J. Hart, Science **339**, 535 (2013).

[3] Q. Zhang, J. Q. Huang, W. Z. Qian, Y. Y. Zhang, F. Wei, Small **9**, 1237 (2013).

[4] Z. Liu, X. Lin, J. Y. Lee, W. Zhang, M. Han, L.M. Gan, Langmuir **18**, 4054 (2002).

[5]Y. Xing, J. Phys. Chem. B **108**, 19255 (2004).

[6] N. Rajalakshmi, H. Ryu, M. M. Shaijumon, S. Ramaprabhu, J. Power Sources **140**, 250 (2005).

[7] Z. Tang, H. Y. Ng, J. Lin, A. T. S. Wee, D. H. C. Chua, J. Electrochem. Soc. **157**, B245 (2010).

[8] H. Tang, J. H. Chen, Z. P. Huang, D. Z. Wang, Z. F. Ren, L. H. Nie, Y. F. Kuang, S. Z. Yao, G. A. Gruver, R. F. Pascoe, H. R. Kunz, Carbon **42**, 191 (2004).

[9] W. Zhang, J. Chen, G. F. Swiegers, Z. F. Ma, G. G. Wallace, Nanoscale **2**, 282 (2010).

[10] J. Willsau, and J. Heitbaum, J. Electroanal. Chem. **161**, 93 (1984).

[11] A. Honji, T. Mori, K. Tamura, Y. Hishimura, J. Electrochem. Soc. **135**, 355 (1988).

[12] A. C. C. Tseung, and S. C. Dhara, Electrochim. Acta **20**, 681 (1975).

[13] G. A. Gruver, R. F. Pascoe, H. R. Kunz, J. Electrochem. Soc. **127**, 1219 (1980).

[14] T. Kunimoto, M. Inaba, Y. Nakayama, K. Ogata, R. Umebayashi, A. Tasaka, Y. Iriyama, T. Abe, Z. Ogumi, J. Power Sources **158**, 1222 (2006).

[15] E. Guilminot, A. Corcella, F. Charlot, F. Maillard, M. Chatenet, J. Electrochem. Soc. **154**, B96 (2007).

[16] T. Okada, Y. Ayata, H. Satou, M. Yuasa, I. Sekine, J. Phys. Chem. B **105**, 6980 (2001).

[17] S. Takenaka, H. Matsumori, K. Nakagawa, H. Matsune, E. Tanabe, M. Kishida, J. Phys. Chem. C **111**, 15133 (2007).

[18] S. Takenaka, H. Miyamoto, Y. Utsunomiya, H. Matsune, M. Kishida, J. Phys. Chem. C **118**, 774 (2014).

[19] C. Terashima, Y. Iwai, S. P. Cho, T. Ueno, N. Zettsu, N. Saito, O. Takai, Int. J. Electrochem. Sci. **8**, 5407 (2013).

[20] J. Kang, O. L. Li, N. Saito, Nanoscale **5**, 6874 (2013).

[21] O. Takai, Pure Appl. Chem. **80**, 2003 (2008).

[22] H. O. L. Li, J. Kang, K. Urashima, N. Saito, J. Inst. Electrostat. Jpn. **37**, 22 (2013).

[23] A. Kongkanand, S. Kuwabata, G. Girishkumar, P. Kamat, Langmuir **22**, 2392 (2006).

[24] Z. Chen, M. Waje, W. Li, Y. Yan, Angew. Chem. Int. Ed. **46**, 4060 (2007).

[25] P. J. Ferreira, G. J. la O, Y. Shao-Horn, D. Morgan, R. Makharia, S. Kocha, H. A. Gasteigerc, J. Electrochem. Soc. **152**, A2256 (2005).

[26] S. Takenaka, H. Miyamoto, Y. Utsunomiya, H. Matsune, E. Tanabe, M. Kishida, J. Electrochem. Soc. **155**, B929 (2008).

[27] X. Li, W. Chen, J. Zhao, W. Xing, Z. Xu, Carbon **43**, 2168 (2005).

[28] Y. Wang, and N. Toshima, J. Phys. Chem. B **101**, 5301 (1997).

[29] Y. Liu, J. Chen, W. Zhang, Z. Ma, G.F. Swiegers, C.O. Too, G.G. Wallace, Chem. Mater. **20**, 2603 (2008).

[30] B. Lim, X. Lu, M. Jiang, P.H.C. Camargo, E.C. Cho, E.P. Lee, Y. Xia, Nano Lett. **8**, 4043 (2008).

Chapter 5

~ Enhanced durability of silica coated Pt/Cs modified by benzoic acid for proton exchange membrane fuel cell application ~

~ Enhanced durability of silica coated Pt/Cs modified by benzoic acid for proton exchange membrane fuel cell application~

5.1 Introduction

Proton exchange membrane fuel cells (PEMFCs) has many advantages because low temperature operation is available, low emissions are generated from this device and this reaction convert to electrical energy with high efficiency [1,2]. In the present, it is well known that the Pt supported on carbon materials are used be commercially catalyst in PEMFC. The dissolution of Pt nanoparticles contributes to deactivation of catalyst in acidic electrolytes [3-6]. The degradation phenomena of catalyst in fuel cell can occur such as Platinum dissolved in acidic electrolyte, Pt nanoparticles moved to together each others to form big particles, Pt nanoparticles removed from carbon support and Ostwald ripening. To solve the problem, the metal elements such as gold, cobalt and palladium which formed with Pt to be alloy catalysts have been studied [7-10].

B. Lim *et al.* found that the alloy between Pd and Pt which formed nanodendrites shape had higher activity than Pt/Cs about two and a half times base on the same amount of Pt. If the activity compared with Pt-black catalyst, the alloy between Pd and Pt which formed nanodendrites shape shows five times.Toda *et al.* investigated Pt alloys which were formed between nickel, cobalt, iron and platinum to determine electrocatalytic activity compared with pure Pt-catalysts. In case of Ni-Pt alloy was found that at content of Ni is approximately 30%, the activity exhibited maximum activity. Moreover, Co-Pt alloy which approximately 40% content of Co showed the maximum activity and the last Fe-Pt alloy was observed at approximately 50% content of Fe had maximum activity. The alloy catalysts have higher activity and durability compared to that of pure Pt catalysts. However, the metal elements which formed with Pt to be alloy catalysts still dissolve in acidic electrolyte at the cathode electrode. The dissolution of the non-noble transition metal also contributes to deactivation of the catalysts. The polymer electrolyte membrane could be deposited from the dissolved metal elements, which membranes will loss ability to transfer proton [11-13].

Silica coated on Platinum/carbons was studied by Takenaka *et al*. to enhance the durability and activity of catalysts [14-17]. The electrochemically active surface area of silica coated Platinum/carbons were higher than that of non-coated Platinum/carbons after durability test. The ORR activity of Platinum/carbons decreased rapidly during the durability test but in case of silica coated Platinum/carbons, the ORR activity was stable at all during the durability test. From these results show that the silica coated Platinum/carbons enhance the durability and the activity of catalyst is quite similar to that of non-coated catalyst. However, the preparation of catalyst needs to use toxic and strong acid (8M H_2SO_4 and 8M HNO_3) to modify carboxyl group on carbon surface due to the carboxyl group is a key for binding APTES on carbon surface [18]. To avoid dissolution of Pt from using strong acid, multiple processes are required in catalyst preparation.

In the present study, commercial Pt/C catalysts were modified in one step process without dissolving Pt catalyst by using benzoic acid in the pH range 2-4 to introduce carboxyl group on carbon surface and covered with silica layers to (1) avoid the agglomeration of the nanoparticles and (2) to prevent Pt nanoparticles removed from carbon supports.. This study is expected to provide an alternative solution for high durability electrode material for PEMFCs.

5.2 Experimental details

5.2.1 Preparation of benzoic acid-modified Pt/Cs

0.01 g Pt/Cs has been sonicated under 10 mL benzoic acid solution (0.005 to 0.02 g benzoic acid in distilled water) for 1 hour. After sonication for 1 hour, the suspension was filtrated by distilled water followed by drying process at 80 $^{\circ}$C for 6 hours.

5.2.2 Preparation of silica coated benzoic acid-modified Pt/Cs

Silica coated benzoic acid-modified Pt/Cs was synthesized by successive hydrolysis of 3-aminopropyltriethoxysilane (APTES) and triethyl orthosilicate (TEOS). In this process, benzoic acid-modified Pt/Cs (0.005 g) was dispersed in distilled water (100 mL) by ultra-sonication for 30 minutes. APTES (50 μL) was added into the solution and then stirred at 60 $^{\circ}$C for 30 min. Subsequently, TEOS (50 μL) was added to the solution. The mixture was stirred for 90 min at 60 $^{\circ}$C. The sample was filtrated and washed several times by distilled water prior to drying at 80 $^{\circ}$C for 6 hours.

5.2.3 Characterization of Catalysts

The morphology and particle size of Pt nanoparticles were examined by transmission electron microscopy (TEM) which were measured in case of before and after silica coating in durability test. The voltage in measurement was accelerated to 200 kV. The TEM images of the samples were recorded with a JEM-2500SE.

Electrochemical measurements, the unit cell which used for electrochemical measurement consists of three electrodes 1) working electrode, 2) counter electrode (Pt wire) and 3) reference electrode (saturated Ag/AgCl electrode). The electrolyte in measurement can be acidic or basic depend on the application of catalyst. Before start cyclic voltammetry (CV) measurement, we have to clean surface of a glassy carbon disk electrode (3 mm diameter) which was used as the substrate for the catalysts (working electrode) by polishing. First the catalyst is dispersed in ethanol, and 5% Nafion using an ultrasonic device about 20 minutes to prepare the catalyst ink. The ink was dropped on the glassy carbon electrode and dried in atmosphere air until the ink is completely dried. The electrolyte was purged under N_2 until 30 minutes. The working electrode was put in acidic solution (0.5 M H_2SO_4) which purged with N_2. The scan rate of potential is fixed at 50 mV s^{-1}. The operation temperature is room temperature. The range of potential is fixed between -0.2 and 1.20 V. Three electrodes are connected to potentiostat device. The samples are measured by CV. Prior to the CV measurement, the catalyst on glassy carbon electrode was cleaned to remove contaminates on catalyst surface by scanning potential between -0.2V to 1.2V for 30 cycles. In case of determination of polarization curve, the working electrode was put in acidic solution (0.5 M H_2SO_4) which purged with O_2. The scan rate of potential and rotation rate of electrode are fixed at 10 mV s^{-1} and 1600 rpm, respectively. The operation temperature is room temperature. The range of potential is fixed between 0.22 V and 1.0V. Three electrodes are connected to potentiostat device. The samples are measured by LSV.

5.3 Results and discussion

5.3.1 Synthesis mechanism of silica-coated Pt/Cs modified by benzoic acid

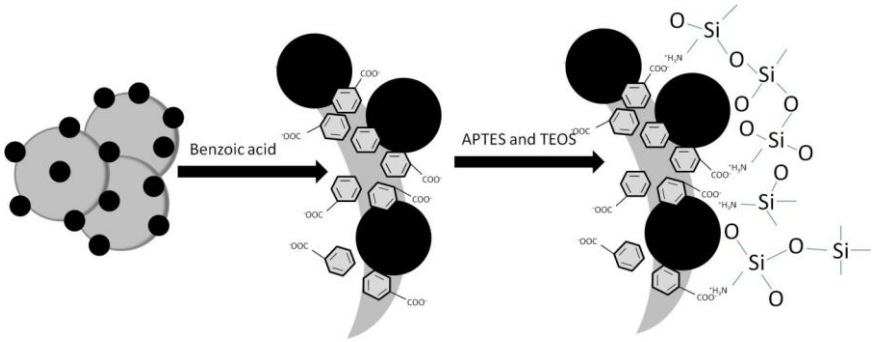

Fig.5.1 Schematic drawing of possible silica coated Pt/Cs mechanism.

The possible mechanism of silica coating is shown in Fig. 5.1. The adsorption of organic compounds on carbon surface was the result of several interactions such as electrostatic bonding, and π-π bonding, etc [19,20]. In case of benzoic acid (Fig. 5.1), benzoic acid could be adsorbed on Pt/Cs with π-π bonding and electrostatic bonding between benzoic acid and Pt/C surface [21-24]. In second step APTES was adsorbed on Pt/Cs due to adhesion force between carboxyl group of benzoic acid and amino group of APTES [18]. APTES behave like the mediator which creates nucleation sites for growing of silica from TEOS [16].

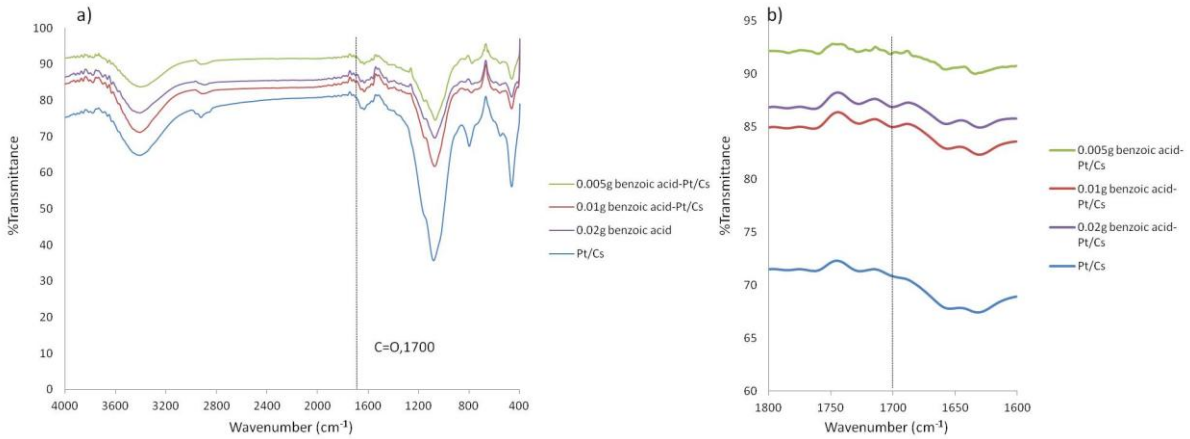

Fig.5.2 FTIR spectra of Pt/Cs, benzoic acid, and benzoic acid-modified Pt/Cs with different amount of benzoic acid in range a) 4000-400, and b) 1800-1600.

The infrared spectrum can conveniently be split into four regions for interpretation: 4000–2500 cm^{-1}: absorption of single bonds to hydrogen such as C–H, O–H, N–H, 2500–2000 cm^{-1}: absorption of triple bonds such as C≡C and C≡N, 2000–1500 cm^{-1}: absorption of double bonds such as C=C, C=O, 1500–400 cm^{-1}: absorption owing to other bond deformations such as rotating, scissoring and some bending [25]. Fig. 5.2 shows FTIR spectra of Pt/Cs, and benzoic acid-modified Pt/Cs with different amount of benzoic acid. Fig. 5.2b, the absorption at approximately 1700 cm^{-1} of benzoic acid is observed, which corresponds to C=O stretching vibration of carboxylic acid group in benzoic acid [26]. The result of FTIR spectra suggested that the benzoic acid is successfully adsorbed on Pt/Cs and the mechanism which was proposed in Fig. 5.1 seems realistic.

5.3.2 Morphology of silica-coated benzoic acid modified-Pt/Cs

Fig. 5.3 shows the TEM images of Pt/Cs and silica coated benzoic acid-modified Pt/Cs prepared at different amount of benzoic acid. The size of metal nanoparticles size in Pt/Cs before silica coating was approximately 3.9∓1.3 nm. The size of Pt nanoparticles after silica coating with 0.005 g, 0.01g, and 0.02g were 4.0∓1.3 nm, 3.9∓1.7 nm, and 3.8∓1.4 nm, respectively. It indicated that the silica coating process by using benzoic acid has no significant effect to Pt particles size of Pt/Cs, no dissolution of Pt and also has similar dispersion of Pt on carbon support.

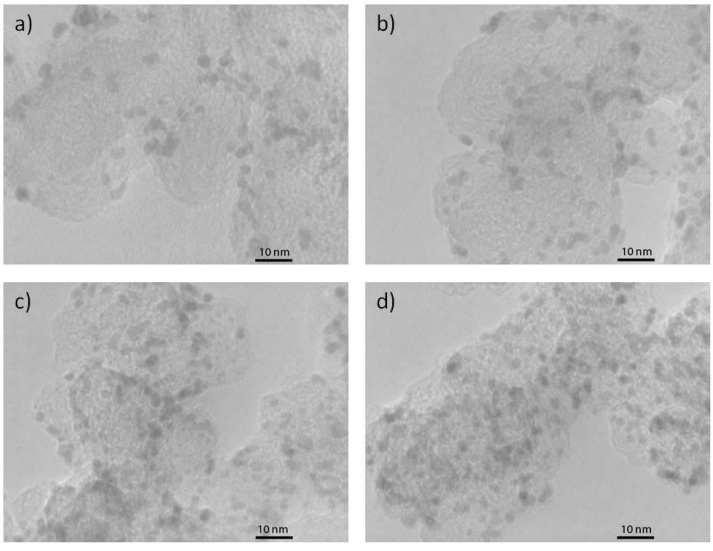

Fig. 5.3 TEM images of a) Pt/Cs before silica coating, b) silica coated benzoic acid-modified Pt/Cs with 0.005g benzoic acid, c) silica coated benzoic acid-modified Pt/Cs with 0.01g benzoic acid, and d) silica coated benzoic acid-modified Pt/Cs with 0.02g benzoic acid.

5.3.3 Electrochemical Analyses

Normally, potential cycling is used to measure the durability of Pt/Cs in acid media solution [27-29]. Fig. 5.4 shows CVs of Pt/Cs and silica coated Pt/C with different amount of benzoic acid during the durability tests. The range of potential of these catalysts was swept between -0.2 and 1.20 V which N_2 purged in acidic electrolyte (0.5 M H_2SO_4). The peak of adsorbed and desorbed hydrogen on Pt surface were found in cyclic voltammogram at -0.2 to 0.1 V and the oxidation and reduction of Pt metal peak also were found in cyclic voltammogram [14-17]. After finish the durability test (500 cycles), the peak current density of Pt/Cs was significantly decreased. These results indicate that Pt metal particles in Pt/Cs were seriously agglomerated and detached from carbon supports in H_2SO_4 electrolyte. On the other hand, similar peak couples were also observed for all silica coated Pt/Cs with different amount of benzoic acid, as observed in Fig. 5.4b-d. For sample coated with 0.005 - 0.02 g benzoic acid with distilled water, the peak currents after 500 cycles for the sample were higher than of non-coated Pt/Cs.

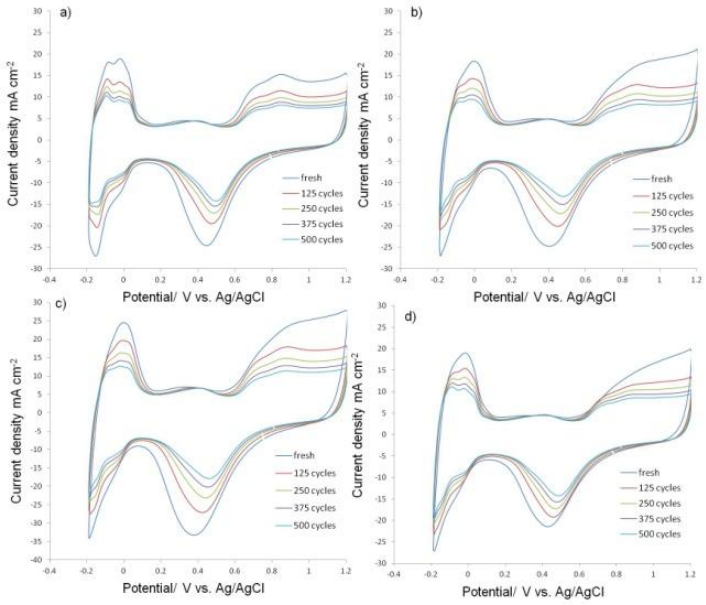

Fig. 5.4 CVs for Pt/Cs and silica coated benzoic acid-modified Pt/Cs with different amount of benzoic acid under N_2-purged 0.5 M H_2SO_4 during the durability tests a) Pt/Cs, b) silica coated with 0.005g benzoic acid, c) silica coated with 0.01g benzoic acid, and d) silica coated with 0.02g benzoic acid.

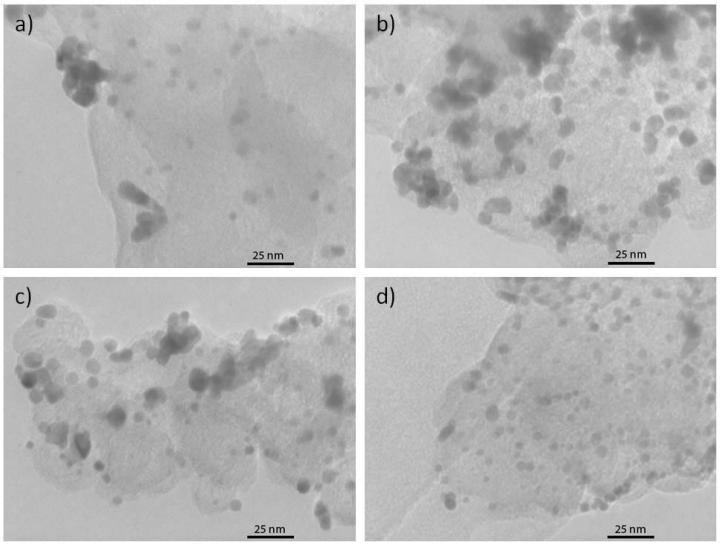

Fig. 5.5 TEM images of a) Pt/Cs, b) silica coated with 0.005g benzoic acid, c) silica coated with 0.01g benzoic acid, and d) silica coated with 0.02g benzoic acid.

Fig. 5.5 (a)-(d) shows the TEM images of Pt/Cs and silica coated Pt/Cs with different amount of benzoic acid after the durability tests. Compared to Fig. 5.3a, which was the image taken before electrochemical analysis, the metal nanoparticles in Pt/Cs (without silica coating) was severely detached and partially agglomerated after 500 cycles. In contrast, silica coated Pt/Cs with different amount of benzoic acid significantly has successfully secured the Pt nanoparticles on carbon supports. However, there is some agglomeration of Pt nanoparticles in case of 0.005 and 0.01 g benzoic acid, as observed in Fig. 5.5(b)-(c). The agglomeration of Pt particles was prevented when Pt/Cs was coated with 0.02 g benzoic acid (Fig. 5.5(d)). These results agreed with Fig 5.4(a)-(d), where the durability of silica coated with 0.02g was highest among all samples.

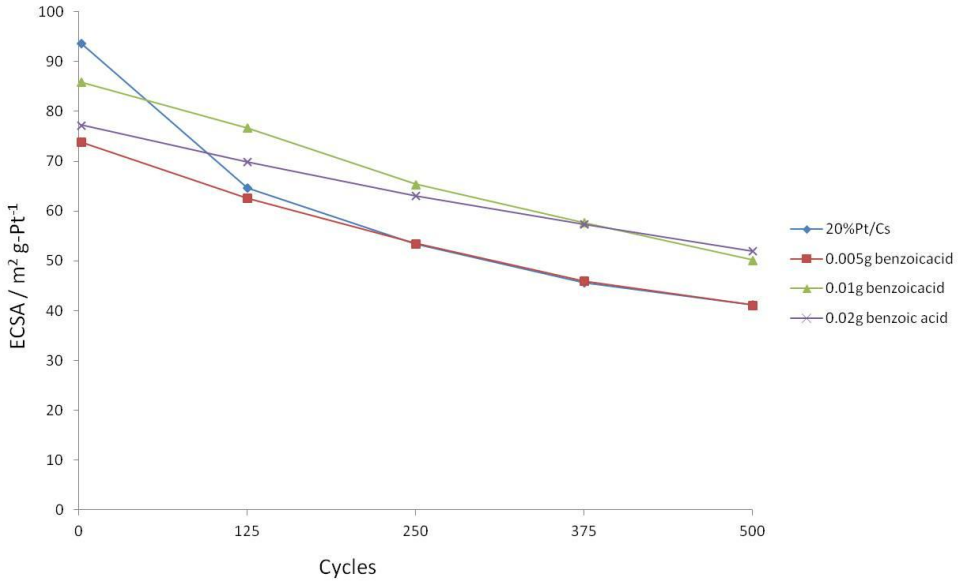

Fig. 5.6 The electrochemically active surface area for Pt/Cs and silica coated Pt/Cs with different amount of benzoic acid during the durability tests.

Figure 5.6 shows the change of ECSA of each Pt catalyst after 500 cycle's tests. The ECSA of Pt/Cs was about 94 m^2 g-Pt^{-1} before testing. The fresh silica coated Pt/Cs-0.005g benzoic acid, silica coated Pt/Cs-0.01g benzoic acid, and silica coated Pt/Cs-0.02g benzoic acid had a smaller ECSA (74, 86, and 77 m^2 g-Pt^{-1}, respectively) than the fresh Pt/CS catalyst. After 500 cycles, ECSA of Pt/Cs was 41 m^2 g-Pt^{-1} and silica coated Pt/Cs with 0.01, 0.02 g benzoic acid had larger ECSA than Pt/Cs (52 and 60 m^2 g-Pt^{-1}, respectively).

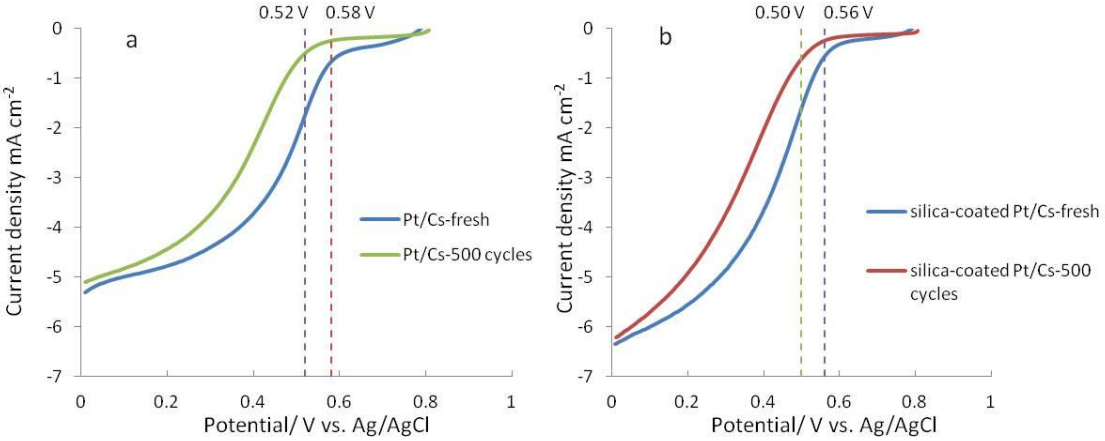

Fig. 5.7 Polarization curves associated with the ORR on Pt/C, and silica coated Pt/Cs with 0.02g benzoic acid in acid a) before and b) after 500 cycle's durability tests

Before the durability test, the ORR onset potential of Pt/Cs and silica coated Pt/Cs with 0.02g benzoic acid in acid were 0.58 V and 0.56 V, respectively. It indicated that the catalytic activity of silica coated Pt/Cs slightly lower than Pt/Cs. After 500 cycles durability test, ORR onset potential of Pt/Cs and silica coated Pt/Cs with 0.02g benzoic acid were 0.52 V and 0.50 V which is shown in Fig 5.7. From both before and after durability test it indicated that the coverage with silica had slightly lower catalytic activity.

The normalized electrochemical surface area (N-ECSA) is the ratio between the electrochemically active surfaces during *n* number of cycles to the initial electrochemically active surface. The N-ECSA values were calculated according to the equation (1).

$$N - ECSA = ECSA\ (cycle\ n)/ECSA\ (\ initial\ cycle) \quad (1)$$

Fig. 2.8 shows hydrogen desorption region which use to determine electrochemically active surface area (ECSA). Due to the exactly amount layer of hydrogen which adsorbed on Pt surface is unknown. So, the calculation of ECSA values based on one layer of hydrogen which adsorbed on Pt surface [30]. The ECSA was calculated using Eq. (2):

$$ECSA = \frac{Q_H}{2.1 \times m_{Pt}} \quad (2)$$

where Q_H is area under peak of desorbed hydrogen from Pt surface (C m^{-2}), 2.1 is the charge required to oxidize a monolayer of hydrogen on the Pt surface (C m^{-2}), and m_{Pt} is the amount of Pt loaded on working electrode (g m^{-2}) [31-33].

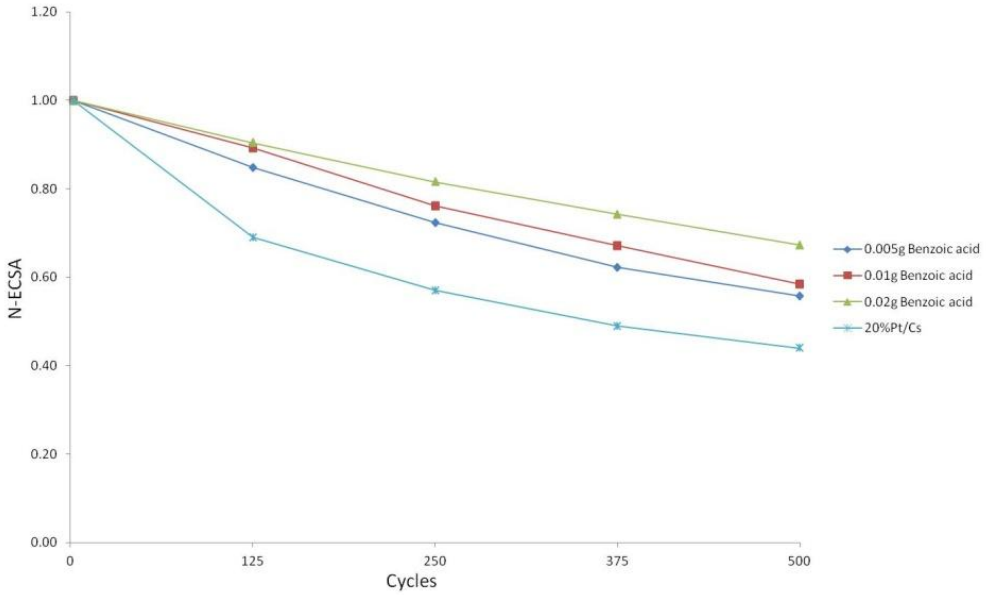

Fig. 5.8 Normalized electrochemical surface area for Pt/Cs and silica coated Pt/Cs with different amount of benzoic acid during the durability tests.

The N-ECSA for fresh Pt/Cs decreased sharply as the number of potential cycles increased, and reduced to 0.44 after 500 cycles. The N-ECSA after 500 cycles for silica coated Pt/Cs with 0.005, 0.01, and 0.02 g benzoic acid was reduced to 0.56, 0.58, and 0.67, respectively. The results showed the durability increased with increasing the amount of benzoic acid. This finding can be explained by the interaction force occurred during the coating process. Due to the increases of adsorption of benzoic acid on Pt/Cs when increase the amount of benzoic acid, the adhesion force between carboxyl group of benzoic acid and amino group of APTES also increased. The silica bonding was strengthened by stronger adhesion force and enhanced the stability of Pt nanoparticles on carbon support.

5.4 Conclusion

Silica coated Pt/Cs modified by benzoic acid catalysts has shown significant improvement in terms of durability under acidic condition. The degree of improvement was highly depended on the amount of benzoic acid. The silica coated Pt/Cs with 0.005, 0.01, and 0.02 g benzoic acid demonstrated an enhancement of durability, respectively, by 12%, 14% and 23% compared to that of non-coated Pt/Cs after 500 CV cycles under 0.5M H_2SO_4 electrolytes. TEM images proved that the silica coating has successfully prevented Pt nanoparticles detach from carbon support and agglomeration between nanoparticles. This innovative coating method is expected to applicable to most of metal based catalysts supported on carbon matrix. It will give an alternative approach to the synthesis of highly durable catalyst for PEMFCs application.

References

[1] M. K. Debe, *Nature,* 2012, 486, 43-51.

[2] J. Wing, M. Ryan, D. Carter, The Fuel Cell Industry Review 1012, *Fuel Cell Today*, Royston, Hertfordshire, UK, 2012

[3] J. Willsau, J. Heitbaum, *J. Electroanal. Chem*., 1984, 161, 93-101.

[4] A. Honji, T. Mori, K. Tamura, Y. Hishimura, *J. Electrochem. Soc*., 1988, 135, 355-359.

[5] A. C. C. Tseung, S. C. Dhara, *Electrochimica Acta*, 1975, 20, 681-683.

[6] G. A. Gruver, R. F. Pascoe, H. R. Kunz, *J. Electrochem. Soc*., 1980, 127, 1219-1224.

[7] T. Toda, H. Igarashi, H. Uchida, M. Watanabe, *J. Electrochem. Soc*., 1999, 146, 3750-3756.

[8] V. R. Stamenkovic, B. S. Mum, M. Arenz, K. J. J. Mayrhofer, C. A. Lucas, G. Wang, P. N. Ross, N. M. Markovic, *Nat. Mater*., 2007, 6, 241-247.

[9] S. Takenaka, A. Hirata, E. Tanabe, H. Matsune, M. Kishida, *J. Catal*., 2010, 274, 228-238.

[10] B. Lim, M. Jiang, P. H. Camargo, E. C. Cho, J. Tao, X. Lu, Y. Zhu, Y. Xia, *Science*, 2009, 324, 1302-1305.

[11] T. Kunimoto, M. Inaba, Y. Nakayama, K. Ogata, R. Umebayashi, A. Tasaka, Y. Iriyama, T. Abe, Z. Ogumi, *J. Power Sources*, 2006, 158, 1222−1228.

[12] E. Guilminot, A. Corcella, F. Charlot, F. Maillard, M. Chatenet, *J. Electrochem. Soc*., 2007, 154, B96−B105.

[13] T. Okada, Y. Ayata, H. Satou, M. Yuasa, I. Sekine, *J. Phys. Chem. B*, 2001, 105, 6980−6986.

[14] S. Takenaka, T. Miyazaki, H. Matsune, M. Kishida, *Catal. Sci. Technol*., 2015, 5, 1133-1142.

[15] S. Takenaka, H. Matsumori, K. Nakagawa, H. Matsune, E. Tanabe, M. Kishida, , *J. Phys. Chem.* C, 2007, 111, 15133-15136.

[16] S. Takenaka, H. Matsumori, H. Matsune, M. Kishida, *Appl. Catal., A*, 2011, 409–410, 248–256.

[17] S. Takenaka, H. Miyamoto, Y. Utsunomiya, H. Matsune, M. Kishida, *J. Phys. Chem.* C, 2014, 118, 774-783.

[18] X. Li, W. Chen, Q. Zhan, L. Dai, *J. Phys. Chem. B,* 2006, *110*, 12621-12625.

[19] B. Pan, B. Xing, *Environ. Sci. Technol.*, 2008, 42 (24), 9005-9013.

[20] K. Yang, B. Xing, *Chem. Rev.* 2010, *110*, 5989–6008.

[21] J. M. Chern, Y. W. Chien, *Ind. Eng. Chem. Res.* 2001, *40*, 3775-3780.

[22] E. Ayranci, N. Hoda, E. Bayram, *J. Colloid Interface Sci*., 2005, 284, 83–88.

[23] V. Pakhre, V. C. Srivastava, *International Conference on Chemical, Civil and Environment engineering*, 2012, 261-265.

[24] S. A. S. Ahmed, R. M. M. Abo El-enin, Th. El-Nabarawy, *Carbon Letters*, 2011, 12, 3, 152-161.

[25] B. Faust, Modern Chemical Techniques: An Essential Reference for Students and Teachers, RSC Plublishing, 1997.

[26] A. E. Segneanu, I. Gozescu, A. Dabici, P. Sfirloaga and Z. Szabadai, Organic Compounds FT-IR Spectroscopy,: J. Uddin (Ed.), Macro To Nano Spectroscopy, InTech, 2012, pp. 145-164.

[27] A. Kongkanand, S. Kuwabata, G. Girishkumar, P. Kamat, *Langmuir*, 2006, 22, 2392-2396.

[28] Z. Chen, M. Waje, W. Li, Y. Yan, *Angew. Chem. Int. Ed.*, 2007, 46, 4060 –4063.

[29] P. J. Ferreira, G. J. la O, Y. Shao-Horn, D. Morgan, R. Makharia, S. Kocha, H. A. Gasteigerc, *J. Electrochem. Soc*., 2005, 152 (11), A2256-2271.

[30] X. Li, W. Chen, J. Zhao, W. Xing, Z. Xu, *Carbon*, 2005, 43, 2168-2174.

[31] Y. Wang, N. Toshima, *J. Phys. Chem. B*, 1997, 101, 5301-5306.

[32] Y. Liu, J. Chen, W. Zhang, Z. Ma, G.F. Swiegers, C.O. Too, G.G. Wallace, *Chem. Mater.*, 2008, 20, 2603-2605.

[33] B. Lim, X. Lu, M. Jiang, P.H.C. Camargo, E.C. Cho, E.P. Lee, Y. Xia, *Nano Lett.*, 2008, 8, 4043-4047.

Chapter 6

~ Summary ~

~ Summary ~

Chapter 1 is written on the introduction of fuel cell and proton exchange membrane fuel cell and path way of catalyst to make more understanding in the overall research.

Chapter 2 provides the experiment details of silica coating process and experiment setup of synthesis of Pt supported on carbon nanotubes to be catalyst in proton exchange membrane fuel cell application.

Chapters 3 to 5 discuss on the enhancement of durability of silica coated Pt/Cs and Pt/CNTs for PEMFC application. The silica coated Pt/Cs was successfully synthesized by sol-gel method with three different surfactant types; cationic surfactant (Cetyltrimethylammonium bromide (CTAB)), anionic surfactant (Sodium dodecylbezenesulfonate (SDBS)) and nonionic surfactant (Pluronic 123 (P123)) which mechanism proposed that the surfactants adsorbed on Pt/Cs with hydrophobic bonding and electrostatic bonding of each surfactant to induce and nucleate silica on Pt/C surface. Silica coated Pt/Cs catalyst with this method has shown improvement of the durability under an acidic condition. The silica coated Pt/CNTs also successfully was synthesized by sol-gel method with the cationic surfactant (Cetyltrimethylammonium bromide (CTAB)). Although Pt/CNTs were not coated by silica, its durability was higher than Pt/Cs during 300 potential cycling test in an acidic electrolyte. After Pt/CNTs was coated by silica, the silica coated Pt/CNTs show higher durability than both non-coated Pt/CNTs and Pt/Cs. On the different way to synthesize silica coated Pt/Cs to prevent the agglomeration of Pt nanoparticles and detachment of Pt nanoparticles from carbon support, Pt/Cs was modified by benzoic acid to generate carboxyl group on Pt/Cs surface. The silica coated Pt/Cs was successfully synthesized in one step without the using of strong and toxic which cause of the dissolution of Pt nanoparticles. Silica coated Pt/Cs modified by benzoic acid catalyst has shown significant improvement in terms of durability under acidic condition during the durability test. The loss of ECSA of silica coated Pt/Cs and Pt/CNTs are summarized in Table 6.1.

Table 6.1: Summary of all the results from this study and compared to the other method from literature reviews.

Catalyst	Method	Loss of ECSA	Cycles test	Ref.
Silica coated Pt/Cs	Sol-gel	~46-55%	500	Chapter 3
Silica coated Pt/CNTs	Sol-gel	~19.0%	300	Chapter 4
Silica coated Pt/Cs modified with benzoic acid	Successive hydrolysis of APTES, TEOS	~33-44%	500	Chapter 5
Silica coated Pt/Cs	Successive hydrolysis of APTES, TEOS	~26.3%	50,000	[1]
Silica coated Pt/CNTs	Successive hydrolysis of APTES, TEOS in present of NH_2-$(CH_2)_n$-NH_2	~7.7%	1,500	[2]
Silica coated Pt/CNTs	Successive hydrolysis of APTES, TEOS	~20.5%	1,300	[3]
Silica coated Pt/CNTs	Successive hydrolysis of APTES, MTEOS	~14.3%	20,000	[4]

From Table 6.1, the enhancement of durability of silica coated Pt/Cs and Pt/CNTs in this study still were not as well as the others. It could possible cause of the weak the interaction reaction between Pt/Cs and Pt/CNTs surface, mediator and silica. So, silica could leave from Pt/Cs and Pt/CNTs surface during operation. The solution of this problem may be solved by using stronger interaction reaction such as covalent bond between reaction between Pt/Cs and Pt/CNTs surface, mediator and silica. This innovative coating method is expected to applicable to most of metal based catalysts supported on carbon matrix. It will give an alternative approach to the synthesis of highly durable catalyst for PEMFCs application.

References

[1] S. Takenaka, H. Matsumori, H. Matsune, M. Kishida, Appl. Catal., A, 2011, **409–410**, 248–256.

[2] S. Takenaka, T. Miyazaki, H. Matsune and M. Kishida, Catal. Sci. Technol., 2015, **5**, 1133-1142.

[3] S. Takenaka, H. Matsumori, K. Nakagawa, H. Matsune, E. Tanabe and M. Kishida, , J. Phys. Chem. C, 2007, **111**, 15133-15136.

[4] S. Takenaka, H. Miyamoto, Y. Utsunomiya, H. Matsune and M. Kishida, J. Phys. Chem. C, 2014, **118**, 774-783.

~ List of achievements ~

~ Achievements ~

List of publication in international journals

1. W. Yaowarat, O. L. Li, and N. Saito, Highly durable silica coated Pt/Cs with different surfactant types for proton exchange membrane fuel cell applications, *RSC Advances*, 5 (2015) 44258-44262.

2. W. Yaowarat, O. L. Li, and N. Saito, High durable silica coated Pt/CNTs for PEMFC application, Japanese Journal of Applied Physics, (Accepted).

3. N. Thongwichit, O. L. Li, W. Yaowarat, N. Saito, and U. Suriyapraphadilok, Adsorption of Carbon Dioxide by Solution Plasma Synthesized Hetero-atom Doped Carbon Nano Spheres, Japanese Journal of Applied Physics, (Accepted).

4. W. Yaowarat, O. L. Li, and N. Saito, Enhanced Durability of Silica Coated Pt/Cs modified by benzoic acid for Proton Exchange Membrane Fuel Cell Application, (Submitted to Electrochimica Acta, Dec, 2015).

List of presentation in international conferences

1. W. Yaowarat, N. Zettsu, and N. Saito, "Preparation of Metal Nanoparticles within Mesoporous Silica via Solution Plasma Process (SPP)" AVS 59th International Symposium and Exhibition, October 28 – November 2, 2012, Tampa, Florida, U.S.A.

2. W. Yaowarat, P. Pootawang, and N. Saito, "Synthesis of Silver Nanoparticle within Mesoporous Silica by Using Solution Plasma Processing" The 13th International Symposium on Biomimetic Materials processing, January 22 - 25, 2013, Takayama, Japan.

3. W. Yaowarat, P. Pootawang, and N. Saito, "Synthesis of Silver Nanoparticle within Mesoporous Silica by Using Solution Plasma Processing" 5th International Symposium on Advanced Plasma Science and its applications for Nitrides and Nanomaterials, January 28 – Febuary 1, 2013, Nagoya, Japan.

4. W. Yaowarat, P. Pootawang, and N. Saito, "Incoporation of Silver Nanoparticle Within Mesoporous Silica by Using Solution Plasma Processing" 6th International Conference on Plasma Nanotechnology and Science, Febuary 2 - 3, 2013, Gifu, Japan.

5. W. Yaowarat, O. L. Li, and N. Saito, "Synthesis of Silica Nanotubes by Carbon Nanotubes/CTAB Templates" International Conference on Surface Engineering, November 18 - 21, 2013, Busan, Korea.

6. W. Yaowarat, O. L. Li, and N. Saito, "Fabrication of silica nanotubes using multi-walled carbon nanotubes as template" 2013 Materials Research Society Fall meeting and Exhibit, December 1 – 6, 2013, Boston, Massachusetts, U.S.A.

7. W. Yaowarat, O. L. Li, and N. Saito, "Preparation of Silica Nanotubes using MWCNTs/CTAB as Templates" 23rd Annual meeting of The Materials Research Society of Japan, December 9 – 11, 2013, Yokohama, Japan.

8. W. Yaowarat, O. L. Li, and N. Saito, "Synthesis of Pt Nanoparticles Supported on CNTs by Solution Plasma Sputtering Processing" 6th International Symposium on Advanced Plasma Science and its applications for Nitrides and Nanomaterials/7th International Conference on Plasma Nanotechnology and Science, March 3 – 6, 2014, Nagoya, Japan.

9. W. Yaowarat, O. L. Li, and N. Saito, "High Durability Silica Coated Pt/CNTs Electrode Material for Polymer Electrolyte Fuel Cell Application" The 15th International Union of Materials Research Societies-International Conference in Asia, August 24 – 30, 2014, Fukuoka, Japan.

10. W. Yaowarat, O. L. Li, and N. Saito, "High durable silica coated Pt/CNT for PEMFC application"7th International Symposium on Advanced Plasma Science and its applications for Nitrides and Nanomaterials/8th International Conference on Plasma Nanotechnology and Science, March 26 – 31, 2015, Nagoya, Japan.

~ *Acknowledgements* ~

This Thesis arose in years of research that has been done since I came to Saito laboratory, Department of Materials, Physics and Energy Engineering, Graduate School of Engineering, Nagoya University. This work would have been impossible without the great supports from many people along the way of my study.

First of all, I would like to express my sincere gratitude to Prof. Nagahiro SAITO (Institute of Innovation of Future Society and Graduate School of Engineering, Nagoya University), who gave me a great chance to study in an excellent place. He provided me an invaluable advice, encouragement, special experiences throughout my work during the study of doctoral course and financial support in first semester of doctoral course. He also inspired me to think and do things in a different way that I have never thought and done before. Thus, this work could not be completed without his supervision.

I would like to deeply thankful to Lecturer Oi Lun Helena LI (Graduate School of Engineering, Nagoya University) and Lecturer Anyarat WATTANAPHANIT (Graduate School of Engineering, Nagoya University) for their valuable guidance and encouragements in my work. These enabled me to develop my thinking and understanding of my research in the right way.

In addition, I am indebted to Prof. Masakuni OZAWA (Institute of Materials and Systems for Sustainability, Nagoya University), Prof. Katsuya TESHIMA (Department of Environmental Science and Technology, Shinshu University) and Assoc. Prof. Yukikazu TAKEOKA (Graduate School of Engineering, Nagoya University) for serving as the thesis committees, whose comments were constructively and especially informative.

I would also express my deepest appreciation to Ms. Eriko KONDO and Ms. Keiko ITO to kindly provide me for all assistances and suggestions during staying in Japan.

I would like to also thank all the members and staffs in SAITO laboratory for all their kind help and a great working environment.

Lastly, I would like to express my sincere thank to my beloved parents, my wife, and my brother for their continuous encouragements and moral supports.

Wattanachai YAOWARAT

Department of Materials, Physics, and Energy Engineering,

Graduate School of Engineering,

Nagoya University

March 2016